1. Introduction.

The rare gases play an important role in electrical discharges of many types, including commercial light sources and laser systems. Their importance rests on their high efficiency of excitation by electron impact into long-lived, energetic atomic and molecular states. An understanding of the mechanisms of creation and destruction of these states is therefore essential to the accurate modelling of these discharges.

In many discharge regimes, the electric field and pressure are such that the electrons approach a state of local equilibrium. Their interaction with the gas particles is then characterised by a number of state parameters which depend only upon the average energy of the electrons. Useful information about these parameters can only be gathered if the strength of the electric field is known - a quantity that is difficult to measure with accuracy. The pre-breakdown discharge between plane parallel electrodes is therefore a useful tool for unravelling fundamental discharge processes because the field strength in this arrangement is uniform and easily calculated. In the past, two principal methods have been used to investigate discharges of this type, namely, measurements of the current passed by the discharge, and measurements of the light given off by the radiative decay of excited states. As described in chapters 2 and 3, measurements of the discharge current can return accurate values of the average number of ions produced by electron collision per unit length of electron travel (known as the primary ionisation coefficient); information of similar quality about the diffusion and destruction of metastable excited states, where these are present, can also be obtained by these techniques. Methods of detection of current which utilise short pulses of excitation permit the values of other electron transport parameters to be measured (eg Nakamura and Kurachi 1988, Dall'Armi *et al* 1992). On the other hand, experiments which measure the light given out by the discharge have a number of advantages. The primary ionisation coefficient can be measured without having to deal with perturbations due to ionisation mechanisms involving excited states (eg Buursen *et al* 1972, Bhattacharya 1976); electron transport parameters, and the rates of creation and destruction of the excited states themselves, can also be determined with increased accuracy (Blevin and Fletcher 1992). Note, however, that some parameters, such as the rates of excitation of energetic states of the rare gases, have remained resistant to measurement by any of these methods.

A third technique which has received much less attention is the detection of excited states by the absorption of light. This has two main disadvantages: firstly, the discharge is

perturbed by the measurement; secondly, the technique is intrinsically noisy, because the noise level is a function of the total light level rather than the small absorption signal. Nevertheless, useful experiments have been performed using optical absorption. For example, many authors have employed the technique to determine the values of the diffusion coefficients and rate of collisional decay of metastable states in the rare, and other, gases (eg Phelps and Molnar 1953, Ellis and Twiddy 1969 and Barbet, Sadeghi and Pebay-Peyroula 1975). More recently, Tachibana (1986) and Tachibana and Phelps (1987), using tuneable lasers as a light source, have measured the excitation coefficient of the argon and neon 1s states by measurements of optical absorption in a pre-breakdown discharge, averaged over the whole discharge. However, the present author is unaware of any attempts to map the distributions of excited states in a pre-breakdown discharge. This is potentially a valuable technique because it allows the simultaneous resolution in both space and time of the concentrations of metastable particles. The greater number of degrees of freedom of such an experiment allows, in principle, more accurate information to be obtained about many of the discharge parameters.

The aim of the present work is the investigation of the possibilities of this technique. The anticipated availability of detailed information about the spatial distribution of excitation in the discharge meant that new, three-dimensional models of the discharge were required in order to analyse the data. Chapters 5 and 6 contain discussions of the treatment of the respective distributions of electrons and metastable excited atoms in this paradigm. Several methods were evolved of solving the coupled equations that describe the concentrations of these particles.

Some theoretical attention has also been paid to aspects of the saturation of the absorption coefficient, the behaviour of metastable states near an absorbing boundary, problems with the analysis of the Molnar experiment, and the effect on the discharge of a radial variation across the cathode of the secondary ejection efficiency.

An experiment was designed which utilised a laser tuned to one of several transitions in argon between states in the 1s and 2p manifolds. Argon was chosen because the wavelength region in which these transitions occur in this gas is suited to the use of inexpensive tuneable semiconductor lasers as a light source. The beam was restricted to a small radius and the optical absorption, integrated along this beam path, was measured as the concentration of metastable particles was modulated. The power was kept to a low level to avoid excessive perturbation of the discharge, and the noise problem was

ameliorated by careful design of the laser control and signal detection apparatus and by the extensive use of signal-averaging and digital filtration techniques. Some preliminary results were obtained which confirm the promise of the method.

Some measurements of the discharge current were also performed. In part these were done in an attempt to obtain accurate values of the primary ionisation coefficient α_i as a function of the average electron energy. This coefficient had not previously been measured in argon using the technique of Haydon and Williams (1976), which allows the contribution made by metastable-produced secondary electrons to be subtracted from the total current. Measurements were made at values of the reduced electric field *E/N* of between 50 and 450 Td (1 Td equals 10^{-17} V cm^2). Below 50 Td, α_i was found to be too small to measure with acceptable precision (see figure 9.6); at the upper end of the range, non-equilibrium effects become important (Kruithof 1940) and it becomes increasingly difficult to apply the Townsend analysis described in chapter 2. The other reason for performing current measurements was to repeat the measurements made by Molnar (1951b) of the effective diffusion and quenching coefficients of argon metastables, for purposes of comparison with a similar determination made by use of the optical absorption technique.

2. Steady state growth of current.

There is a long history of experiments designed to measure the current passed by a pre-breakdown discharge under conditions of varying pressure, potential difference or electrode separation. A class of these experiments involves measurement of the current transmitted by a discharge between plane parallel electrodes as the electrode separation d is varied, while maintaining a constant electric field between the electrodes. This is the so-called spatial growth-of-current or Townsend experiment. In this chapter, Townsend's original theory is reviewed in the light of present knowledge about the effects of excited gaseous particles and the diffusive motions of electrons upon the discharge, and the theoretical expressions necessary to analyse the growth of current experiment are described. Where appropriate, techniques are described for extracting discharge parameters from experimental data by the use of these expressions. Some of the basic physical processes are discussed in section 2.1; the growth of current formula in its simplest useable form is then derived. Two modifications to this expression are considered in the two subsequent sections: in section 2.2, the influence upon the discharge of a significant concentration of excited gas particles is discussed; the last section treats the modifications necessary in the case that the diffusive motion of the electrons cannot be neglected.

2.1. Townsend theory.

The first systematic study of the pre-breakdown discharge was performed by J S Townsend (1902). Townsend found that the increase in current transmitted by a pre-breakdown discharge in a constant, uniform electric field (such as that produced at low current densities between plane parallel electrodes) as the electrodes were drawn apart could, for small separations d, be described by the exponential relation

$$I(d) = I(0)\exp(\alpha_i d) \tag{2.1}$$

where I is the total current and α_i is a constant. Townsend explained this finding by postulating that electrons ejected from the cathode reach an equilibrium state in which the rate of energy loss through inelastic collisions with gas particles is, on average, equal to the rate of gain of energy from the electric field between collisions. The average collision energy of the electrons would then be proportional to the electric field E multiplied by the

distance λ travelled between collisions. Because λ is inversely proportional to the number density N of gas particles, the average collision energy could be expected to be proportional to the quantity E/N, known as the reduced electric field. Owing to the statistical nature of the process, there will always be some fraction of electrons (larger at higher values of E/N) with sufficient kinetic energy to ionize a gas particle upon collision. The stream of electrons would thus be expected to ionize gas particles at a constant rate, producing an exponential increase in the total current with distance from the cathode. The parameter α_i, known as the primary ionization coefficient, can therefore be understood as the average number of ionizing collisions made by an electron in drifting a unit distance toward the anode.

Townsend found that equation (2.1), while satisfactory for low values of the reduced field E/N, did not explain his experimental results at higher values of E/N. In this regime the measured current increased at a rate greater than exponential as the electrodes were drawn apart; a point would eventually be reached where the current would increase through many orders of magnitude, the discharge then becoming self sustained. These phenomena were eventually explained (Holst & Oosterhuis 1923) as being due to the ejection of secondary electrons from the cathode by positive ion bombardment. The Townsend equation, modified to accommodate the production of secondary electrons, becomes

$$I(d) = \frac{I_0 \exp(\alpha_i d)}{1 - \gamma_i \left[\exp(\alpha_i d) - 1\right]} \tag{2.2}$$

where I_0 is the current passed in the limit $d \to 0$ and γ_i, the secondary ionization coefficient, is the average number of secondary electrons ejected from the cathode per ion impact. This equation is much more successful at explaining the growth of current in the Townsend experiment.

Further modifications were required when it was realised that the distance travelled by electrons before reaching equilibrium with the field was, in some cases, not negligible. In this situation there is a layer of gas next to the cathode within which α_i is not a constant. An analysis which does not make this assumption of constancy yields

$$I(d) = \frac{I_0 \exp\left[\int_0^d dz\, \alpha_i(z)\right]}{1 - \gamma_i \int_0^d dz\, \alpha_i(z) \exp\left[\int_0^z ds\, \alpha_i(s)\right]}. \tag{2.3}$$

The variation in α_i is usually confined to a thin 'non-equilibrium' layer at the cathode of thickness d_0'; α_i is approximately constant for $z > d_0'$. This z-dependence of α_i can be approximated, in many discharge regimes, by the step function

$$\alpha_i(z) = \begin{cases} 0, & z < d_0 \\ \alpha_i, & z > d_0, \end{cases} \tag{2.4}$$

where d_0 is defined such that

$$\alpha_i = \frac{1}{d - d_0} \int_0^d dz\, \alpha_i(z), \tag{2.5}$$

without significant error (Haydon and Williams 1973a, b). In this approximation equation (2.3) is replaced by

$$I(d) \approx \frac{I_0 \exp\left[\alpha_i (d - d_0)\right]}{1 - \gamma_i \left\{\exp\left[\alpha_i (d - d_0)\right] - 1\right\}}. \tag{2.6}$$

In those situations where equation (2.6) remains a good approximation, a simple yet powerful analysis due to Gosseries (1939) allows the deduction of α_i and γ_i from measurements of transmitted current at equally spaced values of the electrode separation d. Gosseries showed that $I(d)$, the current measured at spacing d, was related to $I(d+\Delta d)$ by

$$\frac{1}{I(d)} = \frac{1}{I(d + \Delta d)} \exp(\alpha_i \Delta d) + \frac{\gamma_i}{I_0} \left[\exp(\alpha_i \Delta d) - 1\right], \tag{2.6a}$$

where Δd is the increment in the electrode spacing d. The value of α_i may therefore be obtained by plotting $1/I(d)$ against $1/I(d+\Delta d)$.

An extensive discussion of the d_0 approximation, together with an extension to the Gosseries analysis to those cases where it is no longer valid, may be found in Folkard & Haydon (1971a).

As a final point, the Gosseries analysis returns the values of α_i and γ_i/I_0. The secondary coefficient γ_i can therefore be evaluated if the current I_0 is known. However, circumstances may arise in which it is difficult to measure I_0 with accuracy (see chapter 9 for an example). In this case, a plot of $\exp[\alpha_i(d-d_0)]/I(d)$ against $\exp[\alpha_i(d-d_0)]-1$ allows both I_0 and γ_i to be determined, the slope of such a plot being proportional to γ_i/I_0 and the intercept to $1/I_0$. This appears to be a new method.

2.2. Generation of secondary electrons by neutral species.

It was recognised early in the history of studies of pre-breakdown discharges that gas particles in excited states (at least, those with energies larger than the cathode work function) can play a big role in secondary electron generation in some gases (Engstrom and Huxford 1940). This may occur via the radiative decay of the state if the emitted photon strikes the cathode; another mechanism is via the direct collision of the excited atom with the cathode. Although all these processes are known to occur in argon, in practice it is only necessary to take the metastable excited atoms into account when attempting to apply equation (2.6) to the growth-of-current experiment. This difficulty is elaborated in the following two subsections. Section 2.2.3 deals with metastable excited particles reviews some methods which have been used to extract, from the Townsend experiment, information about these particles as generators of secondary electrons.

2.2.1. Photoelectric generation of secondary electrons.

In argon, the $1s_2$ and $1s_4$ states are strongly coupled to the ground state, decaying with lifetimes in the nanosecond range by the emission of photons of wavelength 1048 and 1067 Å respectively. There is no reason to suppose that these states are generated within the discharge volume at a rate which is significantly different to that of the metastable $1s_3$ and $1s_5$ states, which are known to play a significant role (see section 2.2.2 below); there is evidence also that γ_p, the quantum efficiency of ejection of electrons from the cathode by photons, is comparable at these wavelengths to the efficiencies of ejection by ions or excited neutral atoms (see the tables at the end of this chapter). In principle, therefore, these short-wavelength photons might be expected to contribute a significant proportion of the secondary current in the steady-state argon discharge. Because the flux of photons to the cathode is unlikely to be related in a simple way to the electrode separation or gas

pressure, the simple analysis of chapter 2.1 would, in this circumstance, be rendered useless. In practice, effects that can unambiguously be ascribed to photoelectric generation of secondaries are far from obvious. As was said in the introduction to section 2.2, equation (2.6), the modified Townsend equation, is found to be a good predictor of the measured discharge current after the contribution of the metastable states has been subtracted.

Some clues as to an explanation for this discrepancy between expectation and actuality may be found in the γ_p data in table 2.1. Although the value for copper is the only datum that is of direct relevance to the present work, values of the photoelectric efficiency of many metals at $\lambda \sim 1050$ Å have been included. This is because only two measurements could be found for copper, and one of these is of doubtful validity. Data for other surfaces have been included so that the copper value can be seen in context and a better assessment made of its reliability. One notices straight away that there is a considerable spread in the values measured for the same metal by different authors. However, most of the high values have been obtained from experiments *in vacuo*; measurements made in electrical discharges are typically an order of magnitude lower*. Most of the authors who used discharges employed an analysis that did not take into account the phenomenon of radiation trapping, whereas the argon resonant radiation is known to be strongly trapped at pressures greater than about 0.1 Torr (Ellis and Twiddy 1969). It therefore seems that the trapping somehow reduces the effective value of γ_p. The values of γ_p in table 2.1 may be compared with the available γ_m and γ_i data in tables 2.2 and 2.3.

In recent years it has been recognised that the pathway

$$Ar^* + 2Ar \rightarrow Ar_2^* + Ar,$$

$$Ar_2^* \rightarrow 2Ar + h\nu$$

plays a significant role in the decay of both metastable and resonant 1s states at pressures greater than a few Torr (Manzanares and Firestone 1983, and references within). The (vacuum uv) radiation from the decay of the excimer species (thought to be mainly $^{1,3}\Sigma_u^+$ states) is not at a resonant frequency of the ground-state atom and is therefore not

* The exception is the result obtained by Kenty (1933) for Constantan (an alloy of Cu and Ni in the ratio 1:1). The reason for this anomaly is unknown. Note, however, that Kenty's apparatus was maintained at a pressure that was too low for significant trapping to occur.

trapped. The radiative lifetimes of the excimers states are less than 10 μsec (Boucique and Mortier 1970). Photoelectric production by this radiation may be dealt with under two heads. That component produced by the decay of metastable states is separable by the same techniques as the production of secondary electrons by direct collision of metastable particles with the cathode. However the component due to the decay of resonant states is likely, in general, to be as difficult to handle analyically as the $1s_{2,4}$ resonant radiation, for the same reason: the concentration of these atomic states changes with *d* in a non-trivial way, and ought not to be easily separable by time-resolved detection schemes. It is not understood why this phenomenon is observed experimentally to be of negligible significance to the growth-of-current experiment in argon.

2.2.2 Generation of secondary electrons by the flux of excited atoms into the cathode.

Excited particles can be divided into short- and long-lived (ie, metastable) types depending on whether a significant fraction decay to the ground state before diffusing to the cathode. The number densities of short lived states, and therefore the flux of these particles into the cathode, can, by definition, be expected to be negligible. The exception to this rule arises in the case of a strong radiative coupling between the excited and ground states. The effective lifetime of these states may then be lengthened by the phenomenon of radiation trapping. The problem of finding the distributions of resonant states under these circumstances is an intractable one (Holstein 1947) and will not be attempted here. However, the difficulty may be avoided if the effective lifetime of the excited state is significantly longer than the time required for ions to drift between the electrodes. Amies and Fletcher (1983) found this to be true in helium, for example. Unfortunately, this is not the case in argon, the gas that is the main subject of this study. Ellis and Twiddy (1969) found the effective lifetimes (that is, including trapping effects) of the argon resonant $1s_4$ and $1s_2$ states to be about 10^{-4} and 10^{-6} seconds respectively at 1 Torr. These times are comparable to the time taken for Ar^+ ions to drift from anode to cathode (Hornbeck 1951). However, within the discharge regimes that were studied in this work, the concentrations of these resonant 1s states have been found to be orders of magnitude smaller than the concentrations of the metastable $1s_5$ and $1s_3$ states (Ellis and Twiddy 1969, Copley and Lee 1975, Tachibana 1986). It is therefore considered that their contribution to the secondary current by the mechanism of cathodic impact can be neglected.

There are two aspects to consider when attempting to extend the theory of the pre-breakdown discharge to include the generation of secondary electrons at the cathode by the impact of metastable excited states. Firstly, there is the effect this source of secondary electrons has on the analytical tools, described earlier in this chapter, for deducing the values of α_i and γ_i. A method is described in section 3.2 for separating the secondary electrons produced at the cathode by neutrals from those generated by ions, in effect allowing the continued use of the Folkard-Haydon-Gosseries analysis in cases where the contribution of neutral particles is not negligible. Secondly, a complete model of the discharge in these cases must include the contribution of the neutral particles themselves. It is therefore desirable to identify a set of parameters that allow the construction of such a model and to find some method of measuring these parameters. The steady-state concentration of metastable particles, and their effect upon measurements of the DC current passed by the discharge, are discussed in section 2.2.3; methods of measuring some parameters of interest are discussed in chapter 3.

Some measured values of γ_m and γ_i for argon are given in tables 2.2 and 2.3. No γ_i data could be found for copper, so results for a selection of transition metals have been given in both tables for purposes of comparison. There are theoretical reasons for suspecting that the mechanism for ejection of secondary electrons by metastables is similar to that for ejection by ion impact (Hagstrum 1961, Dunning *et al* 1971, Schohl *et al.* 1992). The quantum efficiencies of the two processes might therefore be expected to be comparable. Some support for this hypothesis can be found in the listed values. (See also Borst 1971.) Some of these measurements of γ_i were performed in electrical discharges, but the bulk have been done using beams of ions in a high vacuum. It might be argued that the efficiencies recorded in beam experiments, where the ions typically have energies in the tens of eV, do not extrapolate to the discharge regime, where the ions have energies of fractions of an eV. However, the variation of γ_i with energy in the beam experiments is invariably small. Unless some previously unknown mechanism is operating in the sub-eV range, the extrapolation is felt to be justified.

To sum up sections 2.2.1 and 2.2.2, one may conclude that, although short-wavelength photons and short-lived excited states might be expected to complicate the analysis of the growth-of-current experiment, in practice this is not the case (at least in argon). The reasons for this do not appear to be well understood.

2.2.3. Models of metastable-particle number densities in the steady state.

As was pointed out in the previous two sections, it has been found to be possible in practice to ignore the contributions to the secondary current made by photons and short-lived excited atoms; however, the case of metastable excited atoms is very different. If equations (2.3) or (2.6) are used to analyse experiments performed with a steady source of primary current where there is a strong contribution by metastable particles, the value of the secondary coefficient γ_i appears to vary with d. Haydon & Williams (1973b) recast equation (2.3) in terms of a generalised, spatially varying secondary coefficient $\omega(z)$, giving

$$I(d) = \frac{I_0 \exp\left[\int_0^d dz\, \alpha_i(z)\right]}{1 - \int_0^d dz\, \omega(z) \exp\left[\int_0^z ds\, \alpha_i(s)\right]}. \tag{2.7}$$

This can be changed into a more tractable form by means of another quantity,

$$\overline{\omega}(d) = \frac{\int_0^d dz\, \omega(z) \exp\left[\int_0^z ds\, \alpha_i(s)\right]}{\int_0^d dz \exp\left[\int_0^z ds\, \alpha_i(s)\right]}; \tag{2.8}$$

equation (2.7) then becomes

$$I(d) = \frac{I_0 \exp\left[\int_0^d dz\, \alpha_i(z)\right]}{1 - \overline{\omega}(d) \int_0^d dz \exp\left[\int_0^z ds\, \alpha_i(s)\right]}. \tag{2.9}$$

If the step-function approximation for $\alpha_i(z)$ is used (equation (2.4)), this gives

$$I(d) \approx \frac{I_0 \exp(\alpha_i \Delta d)}{1 - \dfrac{\overline{\omega}(d)}{\alpha_i}\left[\exp(\alpha_i \Delta d) - 1\right]}. \tag{2.10}$$

The application of this equation has been discussed at length by Haydon and Williams (1973a, b). It is, however, worthwhile treating it in some depth here because many of the approximations and expressions that arise are required again in chapters 3 and 4.

The functional form of $\overline{\omega}(d)$ can be predicted under certain circumstances by considering the transport of metastable particles within the discharge volume. The rate of generation of secondary electrons by metastable particles is proportional to f_{mk}, the fraction of metastables created within the discharge which subsequently arrive at the cathode. This quantity may be expressed as

$$f_{\mathrm{mk}}(d) = \frac{\Phi_{\mathrm{m}}(0)}{R} \tag{2.11}$$

where $\Phi_{\mathrm{m}}(z)$ is the total flux of metastable particles flowing toward the cathode through a plane at z and R is the total rate of creation of metastable particles within the discharge volume. The first of these two quantities can be evaluated by recalling that

$$\Phi_{\mathrm{m}}(z) = 2\pi \int_0^\infty dr\, r\, \phi_{\mathrm{m}}(r,z) \tag{2.12}$$

where the flux density $\phi_{\mathrm{m}}(r,z)$ is given by

$$\phi_{\mathrm{m}}(r,z) = D_{\mathrm{m}} \frac{\partial n_{\mathrm{m}}}{\partial z}. \tag{2.13}$$

Provided that radiative coupling with the ground state is not too strong, the number density $n_k(\mathbf{r},t)$ of particles in the kth excited state obeys a diffusion equation of the form

$$\frac{\partial n_k}{\partial t} = D_k \nabla^2 n_k - G_k n_k + w\alpha_k(\mathbf{r}) n_{\mathrm{e}}(\mathbf{r},t) + \sum_{j \neq k} A_{jk} n_j \tag{2.14}$$

where D_k is the diffusion coefficient, G_k is the total volume quenching rate, w is the electron drift speed, α_k is the average number of particles in state k generated per electron per unit distance of travel, n_{e} is the number density of electrons and A_{jk} is the transition rate from the jth excited state. In the case that all the $A_{jk}n_j$ terms are negligible, the sum may be omitted with little error. This was found by Ellis and Twiddy (1969) to be a valid approximation when considering the free decay of the concentrations of argon metastables in afterglow. Equation (2.14) then becomes

$$\frac{\partial n_m}{\partial t} = D_m \nabla^2 n_m - G_m n_m + w\alpha_m(\mathbf{r}) n_e(\mathbf{r},t). \qquad (2.15)$$

As mentioned above, the argon $1s_5$ state is normally present in far greater concentration than the $1s_3$; because of this, the total contribution made by metastable particles to the argon discharge can be calculated to a good approximation by considering the $1s_5$ state alone. Because we are now dealing only with a single metastable state, the numerical subscript '*k*' has been replaced by an 'm' for 'metastable' in equation (2.15). (This convention will be continued whenever the other excited states can be ignored.) Integration of this equation parallel to the cathode plane produces

$$\frac{\partial N_m}{\partial t} = D_m \frac{\partial^2 N_m}{\partial z^2} - G_m N_m + w\alpha_m(z) N_e(z,t) \qquad (2.16)$$

where

$$N(z,t) = 2\pi \int_0^\infty dr\, r\, n(r,z,t) \qquad (2.17)$$

for both metastable particles and electrons. In the limit of negligible diffusion of the electrons, $wN_e(z,t)$ may be replaced by $I(z,t)/e$, where I is the electron current and e is the electronic charge. Within a Townsend discharge in a non-attaching gas such as argon, $I(z,t)$ may be replaced by

$$I(z,t) = I(0,t) \exp\left[\int_0^z ds\, \alpha_i(s)\right], \qquad (2.18)$$

giving

$$\frac{\partial N_m}{\partial t} = D_m \frac{\partial^2 N_m}{\partial z^2} - G_m N_m + \frac{\alpha_m(z)}{e} I(0,t) \exp\left[\int_0^z ds\, \alpha_i(s)\right]. \qquad (2.18a)$$

Equation (2.18) is equivalent to the assumption that electrons drift from cathode to anode at infinite speed. This is a good approximation so far as metastable particles are concerned, because the typical speeds of these particles are orders of magnitude smaller. Some consequences of this difference are discussed in chapter 3, section 3.2.

Solutions to equation (2.16) have been discussed by Davidson (1959), Molnar (1951a) and Haydon and Williams (1973a). Some further approximations must be made

before a closed-form solution can be found. Firstly, let the step-function approximation for $\alpha_i(z)$ given in equation (2.4) be used. This reduces equation (2.18) to

$$I(z,t) = I(0,t)\exp(\alpha_i \Delta z), \qquad z > d_0, \tag{2.19}$$

where $\Delta z = z - d_0$. Secondly, let $\alpha_m(z)$ be approximated in a similar way by

$$\alpha_m(z) \approx \begin{cases} 0, & z < d_0 \\ \alpha_m, & z > d_0. \end{cases} \tag{2.20}$$

Equation (2.18a) can now be written as

$$\frac{\partial N_m}{\partial t} = D_m \frac{\partial^2 N_m}{\partial z^2} - G_m N_m + \frac{\alpha_m}{e} I(0,t)\exp(\alpha_i \Delta z). \tag{2.21}$$

The solution to this equation in the steady state ($\partial N_m / \partial t = 0$, $I(z,t) = I(z)$) is easily shown to be

$$N_m(z) = \frac{\alpha_m I(0)}{D_m e(\mu^2 - \alpha_i^2)} \times \begin{cases} P_1 \cosh(\mu z) + Q_1 \sinh(\mu z), & z < d_0 \\ \exp(\alpha_i \Delta z) + P_2 \cosh(\mu \Delta z) + Q_2 \sinh(\mu \Delta z), & z > d_0 \end{cases} \tag{2.22}$$

where $\mu^2 = G_m / D_m$. The constants P and Q can be evaluated by the application of appropriate boundary conditions (these are discussed in section 3.1.1). The cathodic flux $\Phi_m(0)$ can be evaluated from equation (2.22). This solution was given in a more general form by Haydon and Williams (1973a).

The second quantity, the total rate of creation of metastables, is given by

$$R = w \int_0^d dz\, \alpha_m(z) N_e(z) \tag{2.23}$$

where

$$N_e(z) = 2\pi \int_0^\infty dr\, r\, n_e(r,z). \tag{2.24}$$

If the same approximations used to derive $\Phi_m(0)$ are applied, this becomes

$$R \approx \frac{\alpha_m I(0)}{e\alpha_i}\left[\exp(\alpha_i \Delta d) - 1\right].^* \tag{2.25}$$

The quantity f_{mk} can now be found by use of equation (2.11). Once this quantity is known, an expression for $\overline{\omega}(d)$ can be obtained as follows. The steady-state current density $j(r,0)$ leaving the cathode may be expressed as

$$j(r,0) = j_0(r) + e\gamma_i\phi_i(r,0) + e\sum_k \gamma_k \phi_k(r,0) \tag{2.26}$$

where $j_0(r)$ is the density of primary current, $\phi(r,z)$ represents the flux density of either ions or excited neutral particles toward the cathode through a plane at z and γ_k is the average number of secondary electrons ejected by a gas particle in excited state k that strikes the cathode. If it is again assumed that there is only one metastable state that makes a significant contribution to the cathode current, equation (2.26) may be replaced by

$$j(r,0) \approx j_0(r) + e\gamma_i\phi_i(r,0) + e\gamma_m\phi_m(r,0). \tag{2.27}$$

Integration of equation (2.27) parallel to the cathode plane gives

$$I(0) \approx I_0 + e\gamma_i\Phi_i(0) + e\gamma_m\Phi_m(0). \tag{2.28}$$

The flux $\Phi_i(0)$ of ions at the cathode can be calculated using a procedure similar to that used above in the derivation of R, the difference being that essentially all the ions that are produced in the discharge arrive at the cathode. This flux is therefore given by

$$\Phi_i(0) \approx \frac{I(0)}{e}\left[\exp(\alpha_i \Delta d) - 1\right]. \tag{2.29}$$

Also, from equations (2.11) and (2.25), we have

$$\Phi_m(0) = I(0)\frac{f_{mk}(d)\alpha_m}{e\alpha_i}\left[\exp(\alpha_i \Delta d) - 1\right]. \tag{2.30}$$

---

* Note that R is equal to $\alpha_m\Phi_i(0)/\alpha_i$. The quantity f_{mk} may therefore be viewed as a measure of the ratio between the cathodic flux of metastables and that of the ions.

Substitution of equations (2.29) and (2.30) into equation (2.28) allows an expression for $I(0)$ to be obtained in terms of the fundamental primary and secondary cathodic currents. Comparison of this expression with equation (2.10) allows one to deduce that

$$\overline{\omega}(d) = \alpha_i \gamma_i + \alpha_m \gamma_m f_{mk}(d). \tag{2.31}$$

An alternative representation is

$$\overline{\omega}(d) = \alpha_i \left[\gamma_i \Phi_i(0) + \gamma_m \Phi_m(0)\right] / \Phi_i(0). \tag{2.31a}$$

It can therefore be seen that, subject to many approximations, information about metastables can be deduced by fitting equation (2.10) to experimental measurements of the total current passed by the discharge at varying electrode separations. This approach was used with some success by Haydon & Williams (1973b, 1976) to deduce the value of the product $\alpha_m \gamma_m$ appropriate to the $A^3\Sigma_u^+$ metastable state of the nitrogen molecule.

Time-resolved measurements of current can also be used to gather information about the diffusion and decay rates of metastable particles. This technique is discussed in chapter 3.

2.3. Diffusion of electrons.

A simple random-walk analysis shows that the self-diffusion coefficient of a neutral molecular species is proportional to $\overline{v}\lambda$, where $\overline{v}$ is the average velocity of the molecules and λ is their mean free path (McDaniel 1964a). The motion of charged particles is also characterised by a spread of velocities, so the same analysis should be applicable. The mean velocity of a charged particle is related to the square root of the reduced electric field E/N, whereas the mean free path of any species may be shown to be proportional to $1/N$. The diffusive motion of electrons might therefore be expected to become significant in the limit of low number density N and/or high reduced field E/N. In these regimes, the Townsend growth of current analysis is no longer valid: if the distribution of the electrons is dominated by their own diffusive motion, the current depends in significant part upon the gradient in electron concentration. A quantitative analysis of these effects would require the solution of the electron diffusion equation (Huxley and Crompton 1974)

$$D_L \frac{d^2 N_e}{dz^2} - w\frac{dN_e}{dz} + w\alpha_i(z)N_e = 0, \tag{2.32}$$

where D_L is the longitudinal electron diffusion coefficient and

$$N_e(z) = 2\pi \int_0^\infty dr\, r\, n_e(r,z). \tag{2.33}$$

Chapter 5 contains a discussion of some methods of solving the three-dimensional form of equation (2.32). It suffices to note here that Lucas (1965) has examined the effect of electron diffusion upon the growth of current equation, arriving at the modified form

$$I(d) = \frac{I_0 \exp\left[(\lambda - u)(d - d_e)\right]}{1 - \gamma_i\left\{\exp\left[(\lambda - u)(d - d_e)\right] - 1\right\}} \tag{2.34}$$

where

$$\lambda = \frac{w}{2D_L}, \tag{2.35}$$

$$u^2 = \lambda^2 - 2\alpha_i\lambda \tag{2.36}$$

and

$$d_e = d_0 - \frac{\ln(u/\lambda)}{\lambda - u}. \tag{2.37}$$

This implies that, at values of *E/N* where the diffusion of electrons is significant, the usual Gosseries type analysis will return

$$\lambda - u \approx \alpha_i + \alpha_i^2 D_L / w \tag{2.38}$$

instead of the true value of α_i. Similar conclusions were reached by Huxley (1959), Hurst and Liley (1965), Crompton (1967) and Blevin and Fletcher (1984).

On the following pages, tables have been provided which list some previously published values of the secondary emission coefficients γ_p, γ_m and γ_i. These coefficients are discussed in sections 2.2.1 and 2.2.2 of the present chapter.

Table 2.1. Values of γ_p.

Reference:	Experiment:	Metal:	Heat treatment:	γ_p (%)
Kenty (1933)	A	Constantan	nil	2.0
		W, Ni	~2000 °C, ? min?	0.8
Molnar (1951b)	A	Ta	Yes, but no quant-	0.9
		Mo	itative details given.	0.5
Wainfan *et al* (1953)[a]	B	Ta	nil	5.0
			1000 °C, 10 min	2.5
Colli *et al* (1954)	A	Ni	~1000 °C, 10hr	0.5
Walker *et al* (1955)	B	Cu	nil	4.5
		Cu[b]	700 °C, ? min	1.5
		Ni	nil	5.0
			1000 °C, 1 hr	2.0
		Mo	nil	8.5
			1000 °C, ? min	4.0
Berglund & Spicer (1964)	B	Cu[c]	nil	10.0
Vehse & Arakawa (1969)[a]	B	Ni[d]	nil	3.0

Table headings:

Column 2: the experimental apparatus used can be divided into two types. In type A, γ_p was determined by more or less indirect methods in an electrical discharge in argon. Type B experiments were wavelength-resolved measurements performed in vacuum.

Column 4: In this column is recorded the temperature and duration of any heat treatment applied to the surface.

Notes:

a: The authors' data has been slightly extrapolated to yield a value at the wavelengths of the argon resonance lines.

b: No further change in γ_p was detected after deliberate oxidation of the surface. It therefore seems that the measured value of γ_p for copper is really the value appropriate to the oxide.

c: The surface was coated with a monolayer of Cs. The authors are ambiguous about the effect that this had on their measurements, reporting on the one hand that "the optimum thickness was gauged by maximising the photoelectric yield from a tungsten lamp," but later stating that "the coating had no effect on the photoemission data". The most sensible inference to be made seems to be that the effect was confined to wavelengths much nearer to the photoionisation threshold than are the argon resonance lines.

d: The nickel surface was freshly deposited by evaporation under vacuum. It is interesting that, despite this attempt to ensure the purity of the surface, the shape of the $\gamma_p(\lambda)$ curve obtained by these authors closely matches that obtained from *oxidised* Ni by Walker *et al* (1955).

Table 2.2. Values of γ_m.

Reference:	Type:	Surface:	γ_m (%):	Remarks:
Greene (1950)	A	Mo	<10	Deduced from a measurement of > 90% metastables reflected. Subsequent measurements of very small values for the reflectivity of metastables (eg Conrad *et al* and references within) must cast doubt on this figure.
Molnar (1951b)	A	Ta	~2.3	Estimated by equating γ_m to γ_i.
		Mo	~6.0	Estimated by equating γ_m to γ_i.
Dunning *et al* (1971)	C	Stainless steel	~110	Chemically cleaned surface.
Dunning & Smith (1971)	C	Stainless steel	~100	Chemically cleaned surface.
		Cu	88	Chemically cleaned surface.
		W	8	Heated to 2000 °C for > 20 sec before measurement.
Schohl *et al* (1992)	B	Mo	2.3	Chemically cleaned surface.
			14.4	After heating to 360 K (!)
		Cu + 2% Be	6.5	Chemically cleaned surface.
			25.7	After heating to 360 K.
		Stainless steel	21.7	Chemically cleaned surface.
			21.2	After heating to 360 K.

Table 2.3. Values of γ_i.

Reference:	Type:	Surface:	γ_i (%):	Remarks:
Molnar (1951b)	A	Mo	7.1	Heat treated, but no quantitative details given.
		Ta	2.6	
Varney (1954)	A	Mo	3	$\gamma_i + \gamma_p$. Electrodes brought to red heat and sputtered prior to measurements.
Parker (1954)	B	Ta	0.65	Lowest energy was 2 eV. Surface flashed to 1400 °C before measurement.
Hagstrum (1956a)	B	Mo	12	Lowest energy was 10 eV. Target flashed to 1900 °C before measurement.
Hagstrum (1956b)	B	W	9.5	> 200 eV. Target flashed to 2000 °C.
			3.5	Same surface after 1 hr in 10^{-8} torr N_2.

Experimental type: The experimental apparatus used to determine γ can be divided into three types. In type A, γ was determined by more or less indirect methods in an electrical discharge in argon. In type B experiments, beams of argon atoms or ions were used in a high vacuum. Dunning & Smith (1971) used a third procedure (type C) in which they utilised rates of Penning ionization in a gas cell to determine the flux of metastables.

3. Time-resolved experiments.

Chapter 2 contains a discussion of the 'Townsend' experiment, that is, the measurement of the steady current passed by a pre-breakdown discharge as a function of electrode separation at a constant electric field. It was shown in that chapter that the values of the primary and secondary ionisation coefficients could be deduced fairly easily from such measurements, provided that it was possible to neglect the contribution made by photons to the secondary current. In section 3.2 of the present chapter it is shown that time-resolved measurements of the current passed by the discharge may also yield useful information about the contribution made to the discharge process by metastable excited particles. The particular procedure that is described is usually known as the 'Molnar' experiment because of the contribution made to its analysis by J P Molnar (Molnar 1951a & b). In this experiment, the source of primary current is 'chopped', ie periodically switched on and off. There are other methods of performing time-resolved experiments (eg Hornbeck 1951, Dall'Armi *et al* 1992, Tsurugida & Ikuta 1993) but these have not been described herein because they have not been used in the present study.

There are some difficulties inherent in the analysis of the Molnar experiment: ambiguities are introduced in cases where atoms in more than one excited state is a significant producer of secondary current; even where this is not the case, the analysis is complicated by the need to maintain a potential difference across the electrodes (if this were not done there would be no current to measure). While the potential difference remains non-zero, electrons are continually removed from the vicinity of the cathode and accelerated across the gap, providing a mechanism for the regeneration of metastable particles, and therefore complicating the time-evolution of their concentration. These difficulties arise in a large part because, in the Molnar experiment, measurements are made of only a single variable: the total current. An alternative procedure is to make direct measurements of the concentrations of excited atoms within the discharge volume, by exploiting the interaction between these atoms and tuned laser radiation. There is no need to maintain the potential difference across the electrodes while this is done, and different metastables can be easily distinguished. There are some practical difficulties involved in the performance of these optical measurements, but the analysis is much simpler.

There are two broad classes of optical technique: measurement of the amount of light emitted or the amount absorbed by the excited atoms. Both techniques have been used extensively to examine glow discharges and afterglows. Most of the published results

that are quoted in section 9.2, for example, were performed in this regime. Understandably, due to the lower signal strength involved, there has been much less work done in pre-breakdown. The Flinders University group led by Blevin and Fletcher have made a number of studies of the distribution of excited states in pre-breakdown. This work was reviewed by Blevin and Fletcher (1992). Tachibana (1986) and Tachibana and Phelps (1987) used measurements of the light absorbed by metastable states in, respectively, neon and argon pre-breakdown discharges to deduce values for the excitation coefficients of these states, but did not attempt spatially resolved measurements.

The purpose of the present chapter is to describe the theory that is fundamental to the analysis of both the Molnar and 'optical' experiments. The chapter is organised into two sections, corresponding to the two different experiments. In section 3.1, a simple eigenvalue expansion is used to model the so-called 'free' decay of the population of metastables that occurs after all sources of current are extinguished. In practical terms, this is accomplished by removing the potential difference between the electrodes at the same time that the primary current is extinguished. The conditions at a physical boundary are discussed at some length in this section. It is shown that measurements of the rates of free decay in a discharge of small physical dimension or at low pressure can return information about the probability that a metastable particle will reflect from a surface without suffering a decay to the ground state. Experiments of the Molnar type are discussed in section 3.2. Molnar's original integral equation analysis is presented in section 3.2.1, whereas section 3.2.2 contains a discussion of an alternative method of solution which relies upon the technique of separation of variables. It is shown in this sub-section that Molnar's analysis is inadequate under some discharge conditions.

3.1. Free decay of metastable concentration.

The diffusion and volume decay coefficients of metastable excited states of many gases have been determined by measurement of the decay in the number density of the state in the afterglow of an electrical discharge. These number densities have mostly been measured by optical absorption (see, for example, Phelps and Molnar 1953; Phelps 1959; Ellis and Twiddy 1969; Copley and Lee 1974 and Kolts and Setser 1978), but natural or laser induced fluorescence has also been used (McCoubrey 1954; Wieme and Wieme-Lenaerts 1974; Levron and Phelps 1978 and Tachibana *et al* 1982). The present author

has attempted similar measurements in a pre-breakdown discharge; the results are reported in chapter 10.

In order to analyse the afterglow decay experiment, it is necessary to solve the metastable particle diffusion equation (equation 2.15). With the source term removed, this becomes

$$\frac{\partial n_m}{\partial t} = D_m \nabla^2 n_m - G_m n_m. \tag{3.1}$$

The geometry of the discharge model is illustrated in figure 3.1.

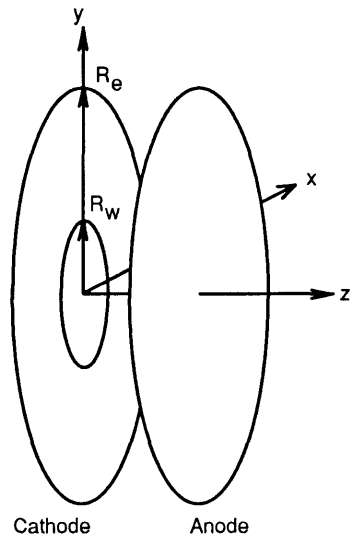

Figure 3.1. The parallel-planar discharge geometry.

The cathode is set parallel to the xy plane at $z = 0$. The primary current is restricted to a circle of radius R_w in the centre of the cathode. The cylindrical symmetry of this arrangement allows all quantities to be expressed as functions of $r = \sqrt{x^2 + y^2}$ and z alone. Equation (3.1), expressed in cylindrical polar coordinates, is

$$\frac{\partial n_m}{\partial t} = D_m \left(\frac{\partial^2 n_m}{\partial z^2} + \frac{\partial^2 n_m}{\partial r^2} + \frac{1}{r} \frac{\partial n_m}{\partial r} \right) - G_m n_m. \tag{3.2}$$

In the present experiment, the radius of the electrodes is several times larger than the electrode separation. In this situation the radial terms in $\nabla^2 n_m$ are small and may be neglected to a good approximation. Equation (3.2) then becomes

$$\frac{\partial n_m}{\partial t} = D_m \frac{\partial^2 n_m}{\partial z^2} - G_m n_m \tag{3.3}$$

(similar to equation (2.16) without the source term). Boundary conditions must be established before this can be solved. These are the subject of the next section.

3.1.1. A new expression for the boundary condition.

The boundary conditions on equation (3.3) are the same as those for the steady-state equation

$$G_m n_m - D_m \frac{\partial^2 n_m}{\partial z^2} = \frac{\alpha_m(z) I(z)}{e}. \tag{3.4}$$

which can be obtained from equation (2.15) by setting the time derivative to zero and neglecting the radial derivatives. Since it is expected that the boundary conditions will be independent of time, the steady-state case is assumed for the remainder of this section.

It is commonly assumed that the number density n_m is zero at a surface, although this is clearly not true if a significant fraction of the metastables that collide with the surface are reflected without relaxing to the ground state. Several authors have independently shown that the correct boundary conditions are of the form

$$n_m(0) - \beta \frac{\partial n_m(0)}{\partial z} = 0 \tag{3.5}$$

and

$$n_m(d) + \beta \frac{\partial n_m(d)}{\partial z} = 0 \tag{3.6}$$

for some constant β (Newton 1948; McCoubrey 1954; Davidson 1959; Lisitsyn *et al* 1970; Sadeghi and Pebay-Peyroula 1974 and Suzuki *et al* 1992). These authors derived expressions for the coefficient β using arguments from the theory of gas kinetics, except for Suzuki *et al* (1992) who used an approximation to a scattering equation borrowed from the theory of radiative transfer. All these expressions contain some dependency upon the reflectivity of the metastable, in such a way that β remains non-zero as the reflectivity

tends to zero. In view of the sometimes severe approximations that were used to derive these formulae, a new analysis was performed.

Before embarking upon this, it is important to point out that the number density of metastable particles will not obey the diffusion equation (3.4) within a distance of about one mean free path from the wall. This is because the validity of the diffusion equation rests on the assumption that the velocities of the metastable particles follow a near-maxwellian distribution. (The velocity distribution cannot be exactly maxwellian because this would imply that the average velocity of the particles, and therefore also their net flux, was exactly zero.) This is unlikely to be true a short distance from an absorbing boundary, since the effect of this boundary is to deplete the proportion of particles that have velocities directed away from the wall. We should therefore define two different number density functions: a 'theoretical' function n_m, representing the solution to the diffusion equation (3.4), and the true number density function n_{true}. These two may be expected to be identical except within about one mean free path of the wall. The forms of n_m and n_{true} near to the wall are illustrated qualitatively in figures 3.2 and 3.3.

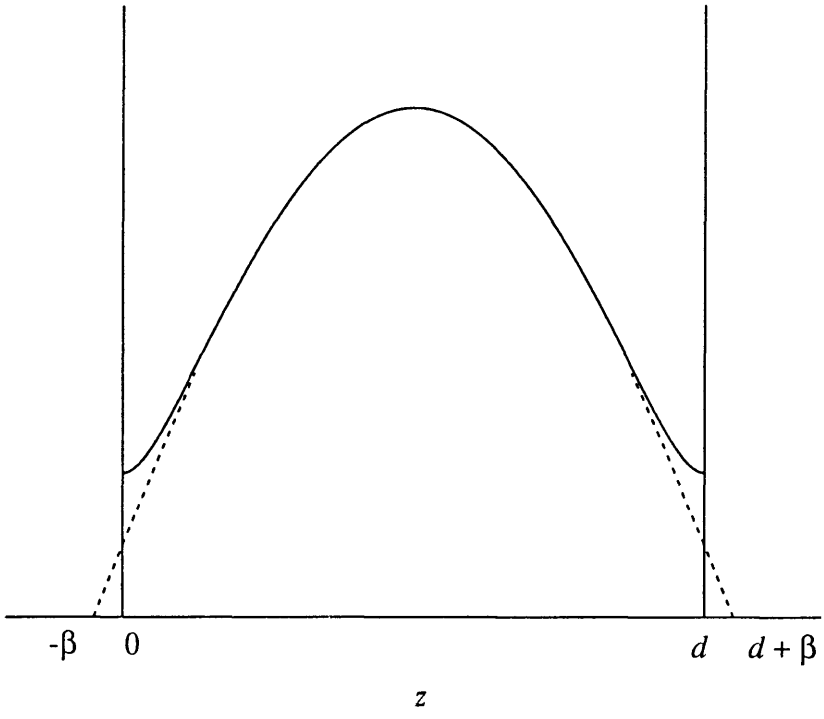

Figure 3.2. The shape of the fundamental decay mode in the case where the concentration at the boundary is nonzero. The solid line represents the estimated shape of the actual concentration $n_{true}(z)$; the dashed line is $n_m(z)$, the solution of the diffusion equation.

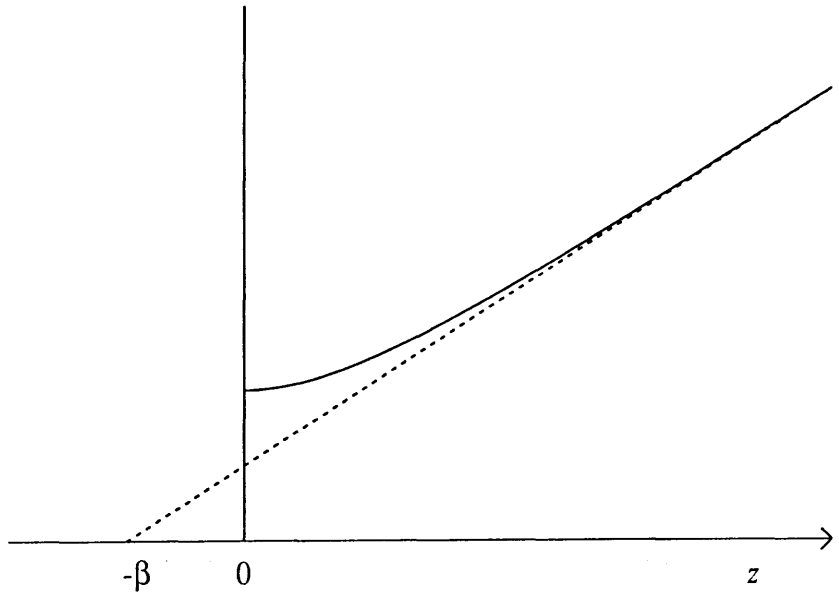

Figure 3.3. The concentration of metastable particles near a surface. The solid line represents the estimated shape of the actual concentration $n_{true}(z)$; the dashed line is $n_m(z)$, the solution of the metastable-particle diffusion equation.

The boundary condition is derived at the cathode, which (see figure 3.1) is located at the $z = 0$ plane. Consider a volume bounded by the cathode on one side and a parallel plane at $z = z'$ on the other. Provided that the characteristic dimension Λ of the container is much larger than the mean free path λ of metastable particles in the gas, z' can be chosen such that $\lambda < z' << \Lambda$. (Note that Λ can be identified with Λ_1, the diffusion length of the fundamental decay mode, which is defined in section 3.1.2.) Metastable particles created in the bulk discharge are assumed to diffuse into this volume through the plane at $z = z'$; some fraction of these will be destroyed at the surface at $z = 0$. It is assumed that there are no other significant sources or sinks of metastables within this volume, implying that $\partial n_m / \partial z$ is approximately constant for $0 < z < z'$. In other words, because $\Lambda >> z'$, it is assumed that the curvature of the solution n_m is very slight over the distance $0 < z < z'$. Lastly, it is assumed that $\partial n_m / \partial y = \partial n_m / \partial z \sim 0$ within the volume. The above approximations should be valid, for example, near a planar electrode in a diffuse discharge through a gas at pressure greater than about 0.01 Torr contained in a chamber of dimensions on the order of centimetres. Given these assumptions, the theoretical number density n_m can be represented to good approximation within the space $0 < z < z'$ by the linear relation

$$n_m(z) \approx k(z + \beta). \tag{3.7}$$

where k and β are constants. Equation (3.7) may be regarded as a line drawn tangent to the solution of the diffusion equation (3.4) at $z = -\beta$.

The boundary condition on equation (3.4) depends on the behaviour near the wall of the actual number density n_{true}. Although a rigorous derivation of n_{true} is difficult, it is shown below that an acceptable approximation can be found. The first step in this analysis is to consider the flow of particles toward the wall. It is convenient to break this flux into a diffusive component and a drift component. Diffusive flow dominates where the only departure from equilibrium is the presence of a concentration gradient; however, as mentioned above, the presence of an absorbing surface may be expected to introduce an asymmetry into the velocity distribution of metastable particles close to the surface. Under these conditions, the particles will have a net velocity and therefore a net 'drift' toward the wall.

An approximate expression for the total flux ϕ toward the wall can be derived using a mean free path analysis similar to that of Chapman and Cowling (1970). To simplify the notation, the following quantities are defined:

$$\bar{v}_{z,+} = \int_0^\infty dv_z \, v_z \, P(v_z) \tag{3.8}$$

and

$$\bar{v}_{z,-} = \int_{-\infty}^0 dv_z \, v_z \, P(v_z) \tag{3.9}$$

where $P(v_z)dv_z$ is the probability that the particle has a z component of velocity between v_z and $v_z + dv_z$. Note that $\bar{v}_z$, the mean z component of velocity, is given by

$$\bar{v}_z = (\bar{v}_{z,+} + \bar{v}_{z,-}). \tag{3.10}$$

Consider first a system at thermal equilibrium in which the concentration of metastable particles is uniform. It is easy to show that

$$\bar{v}_{z,+} = -\bar{v}_{z,-} = \tfrac{1}{4}\bar{v} \tag{3.11}$$

where $\bar{v}$ is the maxwellian mean speed,

$$\bar{v} = \sqrt{\frac{8kT}{\pi m}}, \tag{3.12}$$

and therefore that $\bar{v}_z = 0$. Let us now introduce a concentration gradient. The flux $\phi_+(z)$ of particles crossing from the negative to the positive side of a plane lying normal to the z axis is given by

$$\begin{aligned}\phi_+(z) &= \int_0^\infty dv_z\, v_z\, n_{\text{true}}(z, v_z) \\ &= n_{\text{true}}(z) \int_0^\infty dv_z\, v_z\, P(v_z) \\ &= n_{\text{true}}(z)\bar{v}_{z,+}.\end{aligned} \tag{3.13}$$

Similarly, the flux crossing in the other direction is

$$\phi_-(z) = n_{\text{true}}(z)\bar{v}_{z,-}, \tag{3.14}$$

the net flux $\phi(z)$ being therefore

$$\begin{aligned}\phi(z) &= n_{\text{true}}(z) \times \left(\bar{v}_{z,+} + \bar{v}_{z,-}\right) \\ &= n_{\text{true}}(z)\bar{v}_z\end{aligned} \tag{3.15}$$

The fact that a net diffusive flux can exist where there is a concentration gradient is because $\bar{v}_{z,+}$ is not quite equal to $\bar{v}_{z,-}$ in this case (Langevin 1905). One of the standard routes to Fick's Law is to replace equations (3.13) and (3.14) by the approximations (Chapman and Cowling 1970)

$$\phi_+(z) \approx \left[n_{\text{true}}(z) - u\lambda \frac{\partial n_{\text{true}}}{\partial z} \right] \bar{v}_{z,+} \tag{3.16}$$

and

$$\phi_-(z) \approx \left[n_{\text{true}}(z) + u\lambda \frac{\partial n_{\text{true}}}{\partial z} \right] \bar{v}_{z,-}, \tag{3.17}$$

where u is a number of order unity. The net flux $\phi(z)$ crossing the plane is now given by:

$$\phi(z) \approx n_{\text{true}}(z)\bar{v}_z - u\lambda\left(\bar{v}_{z,+} - \bar{v}_{z,-}\right)\frac{\partial n_{\text{true}}}{\partial z}. \tag{3.18}$$

While the concentration gradient remains the only significant departure from equilibrium, the distribution of velocities among the metastable particles remains maxwellian to a good approximation (Langevin 1905). Application of equation (3.11) annihilates the first term in equation (3.18), which then reduces to Fick's law

$$\phi(z) = -D_{\text{m}}\frac{\partial n_{\text{true}}}{\partial z} \tag{3.19}$$

with the diffusion coefficient D_{m} given by

$$D_{\text{m}} = \tfrac{1}{2}u\lambda\bar{v}. \tag{3.20}$$

The value of u in the last equation has been found to be exactly unity (McDaniel 1964a). Since z' was chosen to be greater than λ, the gas at $z = z'$ may be considered to be sufficiently far from the influence of the surface at $z = 0$ for equation (3.20) to be a good approximation to the flux through the plane at $z = z'$. In other words

$$\phi(z') = -\frac{\lambda\bar{v}}{2}\frac{\partial n_{\text{true}}}{\partial z}\bigg|_{z=z'}. \tag{3.21}$$

Consider now the situation near the partially absorbing surface at $z = 0$. At distances from this surface of the order of one mean free path or less, the velocity distribution cannot be maxwellian, since the effect of the surface is to deplete the population of particles that have velocities with a positive z component. This will give rise to a non-zero value for $\bar{v}_z$. The contribution of the first term in equation (3.18) to the total flux therefore becomes significant as the boundary is approached. Provided that the total flux remains approximately constant in the region $0 < z < z'$ (as it must if there are, as assumed, no other significant sources or sinks of metastable particles in the region), the diffusive contribution must decrease by the same amount. At the wall itself, the diffusive component falls to zero. To see this, consider that, at $z << \lambda$, essentially all the particles with velocities directed toward the wall will go on to collide with it; likewise, metastable particles at this z with velocities directed away from the wall must have just rebounded

without relaxing to the ground state. The net loss flux $\phi(0)$, representing particles that strike the wall and are 'absorbed', ie quenched to the ground state, is the difference between these two fluxes. From equation (3.15), this is equal to

$$\phi(0) = n_{\text{true}}(0)\,\bar{v}_z(0) \tag{3.22}$$

which is the first term in equation (3.18) for $z = 0$. This implies that the diffusive term in equation (3.18), and therefore the concentration gradient $\partial n_{\text{true}}/\partial z$, both fall to zero as $z \rightarrow 0$. Figure 3.2 shows qualitatively the expected shape of $n_{\text{true}}(z)$ near the surface. Note that β has been defined in equation (3.7) so that the boundary condition on equation (3.4) has the required form

$$n_{\text{m}}(0) = \beta \left.\frac{\partial n_{\text{m}}}{\partial z}\right|_{z=0.} \tag{3.23}$$

In order to derive an expression for β, it is necessary to know how $n_{\text{true}}(z)$ varies within the boundary layer and to make some estimates of the distribution of velocities at the surface. The approximation

$$n_{\text{true}}(z) \approx k\left[z + \beta + \lambda \exp(-z/\lambda)\right] \tag{3.24}$$

reproduces the asymptotic behaviour at $z = 0$ (ie, $\partial n_{\text{true}}/\partial z \rightarrow 0$) and $z > z'$ (ie, $n_{\text{true}} \rightarrow n_{\text{m}}$) and also the boundary layer thickness of $\approx \lambda$. Using this approximation to evaluate the fluxes at $z = z'$ and $z = 0$ described by equations (3.21) and (3.22), then equating these fluxes, gives the result

$$\beta \approx -\lambda\left(\frac{\bar{v}}{2\,\bar{v}_z(0)} + 1\right). \tag{3.25}$$

An approximate expression for $\bar{v}_z(0)$ can be found by considering the fraction R of metastable particles that are 'reflected' from the wall without being quenched. Although no data relevant to argon are known, measurements of R for helium metastables incident upon a variety of surfaces have been published by Conrad *et al* (1982a, b). These authors found that the fraction of metastables that were reflected was independent of the angle of incidence. The reflection was found to be specular from clean crystalline palladium, although some non-specular reflection was observed from gas-covered or polycrystalline surfaces. In the absence of more detailed data, we will join with the authors referenced in

the first paragraph of the present section in assuming that R is independent of **v**. In this case, the velocity distribution function $P(v_z)$ of the metastables close to the surface will be of the form

$$P(v_z) = RP(-v_z), \quad v_z > 0. \tag{3.26}$$

It is convenient to define a normalised parent function $P'(v_z)$ so that

$$P(v_z) = \frac{2P'(v_z)}{1+R} \times \begin{cases} R, & v_z > 0 \\ 1, & v_z < 0. \end{cases} \tag{3.27}$$

If the parent distribution P' is assumed to be maxwellian, it can be shown that

$$\bar{v}_z(0) = \frac{(R-1)\bar{v}}{2(1+R)} \tag{3.28}$$

where $\bar{v}$ is the maxwellian mean speed. Substituting equation (3.28) into equation (3.25) gives the final result

$$\beta \approx \frac{2R}{(1-R)}\lambda. \tag{3.29}$$

Table 3.1: Alternative expressions for the coefficient β.

Reference:	β/λ
Newton (1948)	$2(1+R)/3(1-R)$
McCoubrey (1954), Davidson (1959)	$2/(1-R)$
Lisitsyn *et al* (1970), Sadeghi & Pebay-Peyroula (1974)	$(1+R)/(1-R)$
Suzuki *et al* (1992)	$(1+R)/\sqrt{3}(1-R)$
Present work	$2R/(1-R)$

Expressions for β derived by several authors are listed in table 3.1 in terms of the mean free path λ. Where the original expression was couched in terms of the diffusion coefficient, equation (3.20) has been applied with $u = 1$. It can be seen that the expression

derived here is unique in that it gives a value for β equal to zero in the limit of small reflectivity. It is interesting to note that this result is not sensitive to the particular form of approximation to $n_{\text{true}}(z)$ that is used. For example, replacing equation (3.24) by the hyperbolic approximation

$$n_{\text{true}}(z) \approx k\left(\beta + \sqrt{z^2 + \lambda^2}\right) \tag{3.30}$$

leads to an identical result.

In the present section, a mean-free-path analysis has been presented which is perhaps more careful than any previously published. For example, an attempt was made to model the distribution of velocities among the metastable particles near to an absorbing boundary in as realistic a manner as possible. The resulting formula implies that the value of β ought to be close to zero in the case that the fraction of metastable particles which are reflected from the wall is itself small. This is, however, not in accordance with two sets of experimental findings. The first set comprises measurements of the diffusion of metastable particles in the parent gas (eg Futch & Grant 1956, Sadeghi & Pebay-Peyroula 1974); these experiments imply that β for many species is of a size that would argue for a reflectivity of some tens of percent if formulae of the type listed in table 3.1 were accepted as accurate. However, the second class of experiments, which were performed with beams of metastable helium atoms incident upon a range of surface materials (Conrad *et al* 1982a, b) show that only a tiny fraction of these atoms are reflected from the surface without being quenched. The conflict between these two sets of experiments suggests that the problem has not yet been fully understood.

3.1.2. Solutions to the free decay equation.

In order to apply equation (3.29) to decay rate data, it is necessary to solve equation (3.3), which describes the decay in the concentration of metastable particles in an afterglow between infinite parallel planar electrodes. A trial solution of the form $n_{\text{m}}(t,z) = T(t)Z(z)$ allows this equation to be separated into

$$T' = -\nu_k T \tag{3.31}$$

and

$$D_{\text{m}} Z'' = (G_{\text{m}} - \nu_k) Z. \tag{3.32}$$

These have solutions

$$T_k(t) = A_k \exp(-\nu_k t) \tag{3.33}$$

and

$$Z_k(z) = B_k \cos(z/\Lambda_k) + C_k \sin(z/\Lambda_k). \tag{3.34}$$

The general solution is therefore

$$n_m(z,t) = \sum_{k=1}^{\infty} A_k Z_k(z) \exp(-\nu_k t). \tag{3.35}$$

The decay rates ν_k are related to the diffusion lengths Λ_k by

$$\nu_k = \frac{D_m}{\Lambda_k^2} + G_m. \tag{3.36}$$

Further discussion is restricted to the fundamental term in equation (3.35), because this mode becomes dominant late in the afterglow. If the boundary conditions at the cathode and anode are symmetrical, the spatial part of this mode may be expressed as

$$Z_1(z) = \sin\left[\frac{z+\beta}{\Lambda_1}\right] \tag{3.37}$$

where $\Lambda_1 = \pi/(d+2\beta)$. Hence

$$\nu_1 = \frac{\pi^2 D_m}{(d+2\beta)^2} + G_m. \tag{3.40}$$

The coefficients D_m, β and G_m are all functions of the gas number density N and of temperature. Both D_m and β are inversely proportional to N. It is therefore convenient to define new pressure-invariant quantities D'_m and β' such that

$$D'_m = N D_m \tag{3.41}$$

and

$$\beta' = N\beta. \tag{3.42}$$

The dependence of G_m upon N is more complicated. In chapter 4 it is shown that the quadratic expression

$$G_m = \frac{1}{\tau} + \nu_i + C_m N + B_m N^2 \tag{3.43}$$

provides a good description of the volume quenching of argon metastables. In this equation τ is the natural radiative lifetime of the state, ν_i is the rate of quenching by gaseous impurities and C_m and B_m are the two- and three-body collision coefficients respectively. It should be noted that $1/\tau$ for both argon metastables is very small (Small-Warren and Lue-Yung 1975) and can, to a first approximation, be ignored. It was also found to be possible to compensate for the contribution from impurities to some extent (see chapter 9, section 9.4.2).

Equations (3.39) to (3.43) can be used to transform equation (3.36) into a form where the dependence on N is explicit, giving

$$\nu_1 = \frac{\pi^2 D'_m}{N(d+2\beta'/N)^2} + C_m N + B_m N^2. \tag{3.44}$$

At large values of N, this yields

$$\nu_1 \approx B_m N^2; \tag{3.45}$$

in the opposite limit,

$$\nu_1 \rightarrow \frac{\pi^2 D'_m}{4\beta'^2} N. \tag{3.46}$$

In practice, there is often an intermediate range of pressures where

$$\frac{2\beta'}{N} << d \tag{3.47}$$

while at the same time

$$\frac{\pi^2 D'_m}{d^2 N} >> B_m N^2. \tag{3.48}$$

Within this regime,

$$\nu_1 \approx \frac{\pi^2 D'_m}{d^2 N} + C_m N. \tag{3.49}$$

Because the coefficients of the various powers of N often differ by many orders of magnitude, a graph of $\ln(\nu_1)$ against $\ln(N)$ can often be approximated by a series of straight lines with slopes equal to the different powers of N (see, for example, Ellis and

Twiddy 1969). A graph of this type can thus be used to determine the values of the coefficients D'_m, B_m, C_m and β' .

An alternative technique for extracting the parameters D'_m and G_m is to change the electrode spacing d while keeping the pressure constant (eg Molnar 1951b). It can easily be seen from equation (3.44) that, at moderate to high values of N (ie where β is negligible), a graph of ν_1 against π^2/d^2 should yield a straight line with a slope equal to D_m and an intercept equal to G_m. The value of β can also be deduced in this way. Taking another look at equation (3.44), we can see that

$$\sqrt{\frac{1}{\nu_1}} = \left(d + \frac{2\beta'}{N}\right)\sqrt{\frac{N}{\pi^2 D'_m}} \tag{3.50}$$

becomes a valid approximation at low pressures. A plot of $\nu_1^{-1/2}$ against d at constant N should therefore give a straight line with an intercept proportional to β'.

In many ways, it is preferable to extract these parameters by changing the spacing rather than the pressure. Changing the pressure requires that one keep track of the temperature as well, in order to evaluate the gas number density after each change. Changing d is also, on the present apparatus at least, somewhat easier than changing the pressure.

3.2. The Molnar experiment.

Consider a pre-breakdown discharge in which the source of primary current is suddenly switched on. In other words, let $I_0(0,t)$, the primary electron current at the cathode, have the form

$$I_0(0,t) = I_0 H(t - t_{on}) \tag{3.51}$$

where H is the Heaviside function. The total electron current that subsequently leaves the cathode, $I(0,t)$, may be divided into three components, representing contributions respectively from the primary source and the ion- and metastable-induced secondary currents:

$$I(0,t) = I_0 H(t - t_{on}) + e[\gamma_i \Phi_i(0,t) + \gamma_m \Phi_m(0,t)]. \quad (3.52)$$

(The remaining quantities in this equation were defined in chapter 2, section 2.2.3.) Ions and electrons are known to drift much faster than the speed of diffusion of neutral gas particles. The rise in $I(d,t)$ after the primary source is activated will therefore be observed to occur over two very different time scales. The first increase will last for several microseconds, until the distribution of electrons and ions attains a quasi equilibrium state. At this time, nearly all the electrons leaving the cathode have come either from the primary source or from the impact of ions on the cathode; there has not been sufficient time for significant numbers of metastable particles to diffuse back to the cathode. The subsequent rise in current due to metastable-induced secondaries is typically slower by several orders of magnitude. Since only the distribution of metastable particles is of immediate interest, the flux $\Phi_i(0,t)$ of ions onto the cathode may be approximated for this purpose by

$$\Phi_i(0,t) \approx \frac{I(0,t)}{e} \int_0^d dz\, \alpha_i(z) \exp\left[\int_0^z ds\, \alpha_i(s)\right]. \quad (3.53)$$

Substitution of this into equation (3.52) gives

$$I(d,t) = I_{fast}(d,t) + I_{slow}(d,t) \quad (3.54)$$

where

$$I_{fast}(d,t) = I_0 S(d) H(t - t_{on}) \exp\left[\int_0^d dz\, \alpha_i(z)\right], \quad (3.55)$$

$$I_{slow}(d,t) = e\gamma_m \Phi_m(0,t) S(d) \exp\left[\int_0^d dz\, \alpha_i(z)\right] \quad (3.56)$$

and

$$S(d) = \left\{1 - \gamma_i \int_0^d dz\, \alpha_i(z) \exp\left[\int_0^z ds\, \alpha_i(s)\right]\right\}^{-1}. \quad (3.57)$$

Here the relationship between electron currents at the cathode and anode,

$$I(d,t) = I(0,t) \exp\left[\int_0^d dz\, \alpha_i(z)\right], \quad (3.58)$$

has been used. Note also that the amplitudes I_{slow} and I_{fast} of the time-varying currents $I_{slow}(d,t)$ and $I_{fast}(d,t)$ are a measure of the relative contributions of the two processes in the steady-state discharge.

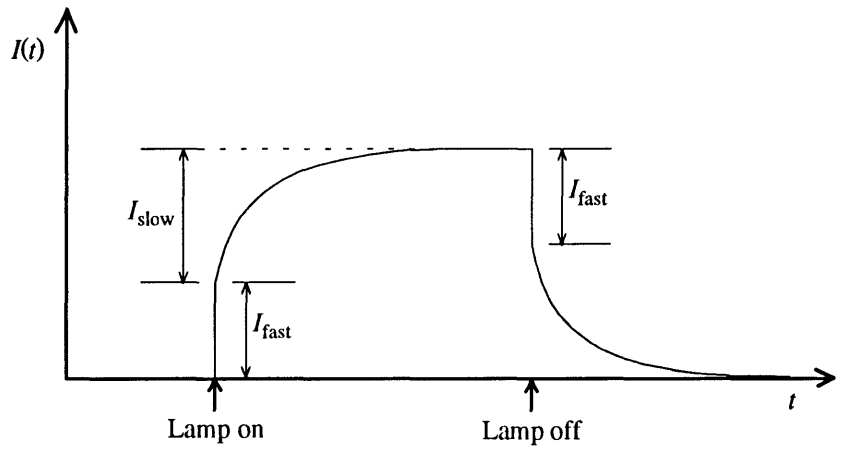

Figure 3.4. The slow and fast components of the rise and decay of current in the Molnar experiment.

A schematic of a typical experimental record of the rise in total current is given in figure 3.4. As this diagram indicates, it is easy to separate the sharp initial rise due to the primary and ion secondary currents from the subsequent slow increase due to the metastable particles. Engstrom and Huxford (1940) were the first to use this technique to examine the contribution made by metastable particles.

Note that, for $t > t_{on}$, equation (3.55) is identical to equation (2.3), which describes the steady-state current in the absence of any metastable contribution. It can therefore be seen that the Folkard-Haydon-Gosseries analysis, described in chapter 2, can still be used in the presence of metastable-induced secondary current by substitution of the amplitude of the fast current rise for the total current in equation (2.3) *et seq.* It is shown in section 3.2.2 that the fall of current after the source of primary current is removed (provided that this has been active for an infinite time beforehand) follows the same form as the rise in current after the source is activated; the size of the fast component can therefore be determined by recording either the rise or decay of the discharge current.

The slow part of the discharge current is, under most circumstances, well described by an infinite series of exponential terms. (Exceptions to this rule will be discussed in sub-section 3.2.2.) The first term is observed to dominate in all but exceptional situations. The

first time constant T_1 is longer than the fundamental-mode free-decay time, being extended by the positive feedback implicit in the generation of secondary electrons by metastables. As electrical breakdown is approached, metastable-induced secondaries form an increasingly large fraction of the total cathode current; modulation of the primary current in this situation amounts to a smaller and smaller perturbation of the system, which becomes correspondingly slower in response. T_1 therefore increases to infinity at breakdown.

The purpose of the remainder of this section is to develop a method of deducing the fundamental free-decay rate ν_1 from measurements of the time constants T_j of the decay of current. Once the free-decay rate is known, the graphical methods described in section 3.1 can be used to evaluate the constants D_m, G_m and β. Two ways to approach the problem of analysis are described below. Both involve the solution of the metastable diffusion equation (equation 2.16), but by use of different methods. In both cases only the rather simple scenario of one active metastable species in an infinite parallel plane geometry will be considered. Although gases with a single metastable state are rare, the approximation remains valid in a number of cases. This is because the population and therefore influence of one state is often greater than that of all the others. This is the case in (unperturbed) neon, argon and probably nitrogen also. Recently, Molnar's theory has been extended to describe those cases in which many metastable states have a significant influence on the discharge (Ernest *et al* 1992). This theory has been applied to an optogalvanic experiment in which the $1s_5$ state of neon is depleted by tuned laser radiation (Ernest *et al* 1992, 1994). In this experiment, the concentration of the neon $1s_5$ state was reduced to a level comparable to that of the $1s_3$ state.

The Molnar analysis may require the measurement of several of the amplitudes and time constants of a series of exponential decays, in the presence of experimental noise. This is known to be an ill-conditioned problem (see, eg, Smith *et al* 1976 and references within). Some techniques of analysis of this type of data are described in section 7.2.3.

3.2.1. Molnar's analysis.

Molnar's approach was to convert the diffusion equation for metastable particles, equation (2.16), into an integral form (Molnar 1951a). To do this, he considered the

generation of metastable particles by an impulse of charge leaving the cathode at time $t = t'$. This may be modelled by inserting a source term in equation (2.21) of the form

$$I(0,t) = \delta(t - t') \tag{3.59}$$

The subsequent free decay of the metastable distribution is a solution of the homogeneous equation (3.3) and therefore is given by an exponential series

$$N_{\mathrm{m}}(z,t) = \sum_{k=1}^{\infty} A_k \sin\left(\frac{k\pi z}{d}\right) \exp\left[-\nu_k (t - t')\right], \quad t > t', \tag{3.60}$$

where the decay rates ν_k are related to the diffusion and quenching coefficients by equation (3.36). (Note that the boundary parameter β has here been assumed to be negligible.) The flux of metastable particles into the cathode in response to this impulse is therefore given by

$$\Phi_{\mathrm{impulse}}(0, t - t') = H(t - t') \sum_k P_k \exp\left[-\nu_k (t - t')\right] \tag{3.61}$$

where

$$P_k = D_{\mathrm{m}} A_k \frac{k\pi}{d}. \tag{3.62}$$

The total flux of metastable particles into the cathode $\Phi_{\mathrm{m}}(0,t)$ in response to a general cathode current $I(0,t)$ can therefore be written

$$\Phi_{\mathrm{m}}(0,t) = \frac{1}{e} \int_{-\infty}^{t} dt' \, I(0,t') \Phi_{\mathrm{impulse}}(0, t - t'). \tag{3.63}$$

The response to a primary current $I_0(t)$ that is turned on at time $t = 0$ can be deduced by breaking the cathode current $I_0(0,t)$ in equation (3.63) into its fast and slow components, as specified by equations (3.58) and (3.54) to (3.57); the result is then inserted into equation (3.56). This gives the following integral equation in the slow current:

$$I_{\mathrm{slow}}(0,t) = \gamma_{\mathrm{m}} S(d) \int_0^t dt' \left[I_0 S(d) + I_{\mathrm{slow}}(0,t')\right] \sum_k P_k \exp\left[-\nu_k (t - t')\right]. \tag{3.64}$$

This equation can be shown to have the solution

$$I_{\text{slow}}(0,t) = I_{s,0} - \sum_{j=1}^{\infty} I_{s,j} \exp\left(-t/T_j\right). \tag{3.65}$$

Insertion of this equation into equation (3.64) gives three sets of equations:

$$\gamma_m \left[I_0 S(d) + I_{s,0}\right] S(d) \sum_k \frac{P_k}{\nu_k} = I_{s,0}; \tag{3.66}$$

$$\gamma_m S(d) \sum_k \frac{P_k}{\nu_k - 1/T_j} = 1 \tag{3.67}$$

for all j;

$$\frac{I_0 S(d) + I_{s,0}}{\nu_k} - \sum_j \frac{I_{s,j}}{\nu_k - 1/T_j} = 0 \tag{3.68}$$

for all k. Also, from the physics of the situation, one can write

$$I_{s,0} = \sum_{j=1}^{\infty} I_{s,j}. \tag{3.69}$$

The time constants T_j can be approximated, provided the P_k, ν_k etc are known, by truncating the infinite series in equation (3.67) at a convenient place and then finding the roots of the resulting polynomial. Once these values are known, it is straightforward to obtain the amplitudes $I_{s,j}$ from a similarly truncated approximation to equation (3.68).

Molnar argued that the amplitudes of terms higher than the second are generally very small. (An exception to this rule will be discussed in the next sub-section.) This comes about mainly because the values of the Fourier coefficients A_k in equation (3.60) decrease rapidly with k, this rapid convergence being a result of the 'smoothness' of the steady-state distribution of metastable particles across the discharge gap. The series of equations (3.66) to (3.69) may therefore be truncated after $j = k = 2$ without significant error. By truncating at this point, and using the approximation $T_2 \sim 1/\nu_2$, Molnar obtained the relation

$$\nu_1 = \frac{I_0 S(d) + I_{s,1} + I_{s,2}\rho/(\rho-1)}{T_1\left[I_0 S(d) + I_{s,2}\rho/(\rho-1)\right]}. \tag{3.70}$$

Here $\rho = \nu_2/\nu_1$. At low pressures, diffusion predominates over volume destruction; under these circumstances ρ is approximately equal to 4. However, if the amplitude of the second component $I_{s,2}$ is small compared to the fast component $I_0 S(d)$, the cruder approximation

$$\nu_1 T_1 \sim \frac{I_0 S(d) + I_{s,0}}{I_0 S(d)} \tag{3.71}$$

may be adequate. Note that the value of ρ approaches unity in the high pressure limit. In this case the following equation may be more useful:

$$\nu_1 T_1 \sim 1 - \frac{I_{s,1}}{I_{s,2}}\left(1 - \frac{1}{\rho}\right). \tag{3.72}$$

In both the high and low pressure cases a more accurate value of ρ could be obtained by use of an iterative procedure.

3.2.2 New results obtained using the method of separation of variables.

Molnar's analysis of the form of the slow portion of the total discharge current is discussed in the previous sub-section. In the present sub-section, an alternative approach is explored, using the technique of separation of variables (SOV). This approach is similar to that of Newton (1948) (except that Newton did not take into account the volume quenching of metastable particles) and Ernest (1995a). The separation method is discussed here because it serves to complement Molnar's integral equation approach. Each method has its respective advantages and disadvantages. Whereas Molnar's method provides approximate values of the current-decay time constants T_j, the separation method permits the calculation of accurate values. The SOV approach requires the use of numerical methods to evaluate the time constants, because these are related to the solutions of a transcendental equation. This is unnecessary within the Molnar formulation, provided that the slowly-varying part of the current (equation 3.65) is approximated by less than five exponentials, because the T_j are then the roots of a polynomial (equation 3.67) of order less than 5. The retention of more terms of equation (3.65) presents problems, however.

The zeros of equation (3.67) can be found numerically, but calculations involving a polynomial of high order can become intractable at large values of the independent variable. Nor is it easy to discern, from equation (3.67), the general trend of the zeros as j grows large. However, this information arises in a natural manner during the SOV analysis. On the other hand, Molnar was able to derive an approximate inversion formula (equation 3.70), which permits the fundamental free-decay rate ν_1 to be determined. No such simple formula can be obtained from the SOV analysis; the ratio between the free-decay rate and the rate of decay of the slow current must be obtained on a case-by-case basis by use of a fairly complicated numerical procedure.

Ernest (1995a) appears to have been the first to recognise that there are circumstances in which some of the decay rates in equation (3.65) may be complex-valued. Neither Molnar or Newton (1948) mentioned the possibility, although nothing in their analyses formally precludes the existence of complex-valued rates of decay. For example, there is nothing to prevent the occurrence of complex roots in the polynomial equation (3.67) (Molnar's equation 18), when terms of order greater than 1 are retained. The two earlier authors may have discounted the possibility on the grounds that such solutions were non-physical. As is shown below, and also by Ernest, that turns out not to be the case.

3.2.2.1. Equivalence of the rise and fall signals.

Molnar discussed the rise in slow current after the initiation of the primary current I_0; in the SOV analysis it is more convenient to treat the decay of slow current after the primary source is extinguished. However, the decay of slow current in a real experiment is observed to have the same shape as the slow current rise after the primary source is turned on. It is here shown formally that the shapes of the current rise and fall are identical. Consider first the situation after the primary current source (which is assumed to have been on for an infinite past time) is extinguished. In this case, equation (2.18a) reduces to

$$\frac{\partial N_{\mathrm{m}}}{\partial \mathrm{t}} = D_{\mathrm{m}} \frac{\partial^2 N_{\mathrm{m}}}{\partial z^2} - G_{\mathrm{m}} N_{\mathrm{m}} + D_{\mathrm{m}} \alpha_{\mathrm{m}} \gamma_{\mathrm{m}} S(d) \exp\left[\int_0^z ds\, \alpha_{\mathrm{i}}(s)\right] \frac{\partial N_{\mathrm{m}}}{\partial z}\bigg|_{z=0.} \qquad (3.73)$$

On the other hand, the concentration of metastables, after the primary source is turned on, obeys the equation

$$\frac{\partial N_m}{\partial t} = D_m \frac{\partial^2 N_m}{\partial z^2} - G_m N_m + \alpha_m \left(\frac{I_0}{e} + D_m \gamma_m \frac{\partial N_m}{\partial z}\bigg|_{z=0} \right) S(d) \exp\left[\int_0^z ds\, \alpha_i(s) \right]. \quad (3.74)$$

However, once equilibrium conditions have been reached, the equilibrium concentration $N_{equ}(z)$ is a solution of

$$0 = D_m \frac{\partial^2 N_{equ}}{\partial z^2} - G_m N_{equ} + \alpha_m \left(\frac{I_0}{e} + D_m \gamma_m \frac{\partial N_{equ}}{\partial z}\bigg|_{z=0} \right) S(d) \exp\left[\int_0^z ds\, \alpha_i(s) \right]. \quad (3.75)$$

Subtraction of (3.74) from (3.75) yields

$$\frac{\partial M}{\partial t} = D_m \frac{\partial^2 M}{\partial z^2} - G_m M + D_m \alpha_m \gamma_m S(d) \exp\left[\int_0^z ds\, \alpha_i(s) \right] \frac{\partial M}{\partial z}\bigg|_{z=0} \quad (3.76)$$

where $M(z,t)$ is defined to be $N_{equ}(z)$ - $N_m(z,t)$. This is identical to equation (3.73).

Having settled this point, a solution of equation (3.73) can be attempted.

3.2.2.2. General solution of the time-dependent diffusion equation after the primary current is extinguished.

Substitution of $N_m(z,t) = Z(z)\Theta(t)$ into equation (3.73) allows its separation into

$$\Theta'(t) = -\Theta(t)/T \quad (3.77)$$

and

$$Z''(z) + \alpha_m(z)\gamma_m S(d) \exp\left[\int_0^z ds\, \alpha_i(s) \right] Z'(0) = \omega^2 Z(z), \quad (3.78)$$

where T is the variable of separation,

$$\omega^2 = \mu^2 - 1/(D_m T) \quad (3.79)$$

and $\mu^2 = G_m/D_m$ as in section 2.2.3. Equation (3.77) has the solution

$$\Theta(t) = \Theta(0)\exp(-t/T). \tag{3.80}$$

Equation (3.78) is an eigenvalue equation which, when solved, may be expected to yield a spectrum of decay time constants T_k. The general solution $N_m(z,t)$ will therefore be of the form

$$N_m(z,t) = \sum_{j=1}^{\infty} Z_j(z)\Theta_j(t)$$

$$= \sum_{j=1}^{\infty} B_j Z_j(z)\exp\left(-t/T_j\right) \tag{3.81}$$

where the $B_j = \Theta_j(0)$ are constants. By use of equations (2.12) (2.13) and (2.28), the form of the 'slow' current can be shown to be

$$I_{slow}(d,t) = \sum_{j=1}^{\infty} I_{s,j}(d)\exp\left(-t/T_j\right) \tag{3.82}$$

where

$$I_{s,j}(d) = S(d)\exp\left[\int_0^d ds\,\alpha_i(s)\right] e\gamma_m D_m B_j Z_j'(0). \tag{3.83}$$

The amplitudes $I_{s,j}(d)$ can be evaluated either from equation (3.68) or by expanding the steady-state concentration of metastables $N_m(z)$ in the eigenfunctions Z_j.

It is not easy to find closed-form solutions to equation (3.78) if the functions $\alpha_i(z)$ and $\alpha_m(z)$ have a non-trivial form. The equation can, however, be converted to an integral form, from which the eigenvalues ω_j can be extracted by numerical methods. This is done as follows. Firstly, the Green's function $g(z,z')$ for equation (3.78) is

$$g(z,z') = \frac{1}{\omega\sinh(\omega d)} \times \begin{cases} \sinh(\omega z)\sinh(\omega d - \omega z'), & z < z' \\ \sinh(\omega z')\sinh(\omega d - \omega z), & z > z'. \end{cases} \tag{3.84}$$

By Green's theorem,

$$Z(z) = Z'(0)\gamma_m S(d)\int_0^d dz'\, g(z,z')\alpha_m(z')\exp\left[\int_0^{z'} ds\,\alpha_i(s)\right]. \tag{3.85}$$

By differentiating with respect to z and then setting $z = 0$, the final result

$$\sinh(\omega d) = \gamma_m S(d) \int_0^d dz' \sinh(\omega d - \omega z') \alpha_m(z') \exp\left[\int_0^{z'} ds\, \alpha_i(s)\right] \qquad (3.86)$$

is obtained. In the general case that ω is complex-valued, this integral will also be complex. Note that, if ω is a solution, then so is $\pm\omega^*$.

3.2.2.3. An approximate case.

Useful, if approximate, information about the behaviour of the eigenvalues ω_j of equation (3.78) can be obtained by considering simple approximations to $\alpha_i(z)$ and $\alpha_m(z)$. Although equation (3.78) can be solved in closed form if the usual step-function approximations are made, for the time being the simplest possible form will be used, which is obtained by setting equal to zero the value of d_0 which occurs in equations (2.4) and (2.20). Equation (3.78) then has the solution

$$Z(z) = \exp(\alpha_i z) + P\cosh(\omega z) + Q\sinh(\omega z), \qquad (3.87)$$

provided that $\omega^2 \neq \alpha_i^2$. If $\omega^2 = \alpha_i^2$, the solution becomes

$$Z(z) = \left\{1 + \left[\exp(-2\alpha_i d) - 1\right]\frac{z}{d}\right\}\exp(\alpha_i z) - \exp(-\alpha_i z). \qquad (3.88)$$

This special case is not further discussed here.

The coefficients P and Q in equation (3.87) may be evaluated by application of the appropriate boundary conditions. Again, for the sake of simplicity, it is assumed that β in equation (3.23) is equal to zero; in other words, it is assumed that the boundary conditions may be approximated by $Z(0) = Z(d) = 0$. In that case, P = -1 and

$$Q = \frac{\cosh(\omega d) - \exp(\alpha_i d)}{\sinh(\omega d)}. \qquad (3.89)$$

Substitution of equation (3.87) into equation (3.78) gives an alternative expression for Q:

$$Q = \frac{1}{\omega}\left[\frac{\omega^2 - \alpha_i^2}{\alpha_m \gamma_m S(d)} - \alpha_i\right]. \tag{3.90}$$

By analysis of the steady-state discharge, it can be shown that

$$\alpha_m \gamma_m S(d) = \frac{\left(\mu^2 - \alpha_i^2\right) I_{slow}/I}{\alpha_i + \mu\left[\cosh(\mu d) - e^{\alpha_i d}\right]/\sinh(\mu d)} \tag{3.91}$$

where the total current $I = I_{fast} + I_{slow}$ (I_{fast} and I_{slow} being the amplitudes respectively of the fast and slow portions of the current decay).

If the parameter ω is allowed to vary continuously, equations (3.89) and (3.90) describe two different functions. To avoid confusion, let us call these Q_1, as defined by equation (3.89), and Q_2, defined by (3.90). The allowed values or eigenvalues of ω are therefore those for which $Q_1 = Q_2$. Alternatively, these eigenvalues can be expressed as zeros of various functions, for example ωQ_1 - ωQ_2, or $1/Q_1$ - $1/Q_2$, depending upon convenience. Figures 3.5 and 3.6 on the next page show, in three dimensions, the variation across the complex plane of the function $\mathfrak{F}(\omega) = 1/Q_1(\omega) - 1/Q_2(\omega)$. These two figures show, respectively, the real and imaginary parts of $\mathfrak{F}$. At the base of each figure is a two-dimensional plot of the values of ω for which Re($\mathfrak{F}$) or Im($\mathfrak{F}$) is equal to zero. The eigenvalues ω_j are those values of ω at which these two sets of lines cross (see figure 4 in Ernest 1995a).

The parameters which were used to calculate these curves are appropriate to a discharge in argon at a reduced electric field E/N of 6.0×10^{-15} V cm^2, a gas number density N of 3.2×10^{16} cm^{-3} (equivalent to about 1 Torr at 300 K) and an electrode spacing of 1 cm. Appropriate values of D_m, G_m and α_i were taken from Ellis & Twiddy (1969) and Kruithof (1940). The breakdown parameter $\chi = I_{slow}/I$ has here been given the value of 0.4. Clearly, at this value of χ, all the eigenvalues ω_j are imaginary. From equation (3.79), it can be seen that these correspond to real values of T. (Because T is a function of the square of ω, the eigenvalues are degenerate with respect to sign.) The absence of other eigenvalues farther out on the complex plane can be confirmed by examining the asymptotic forms of the real and imaginary parts of $\mathfrak{F}$.

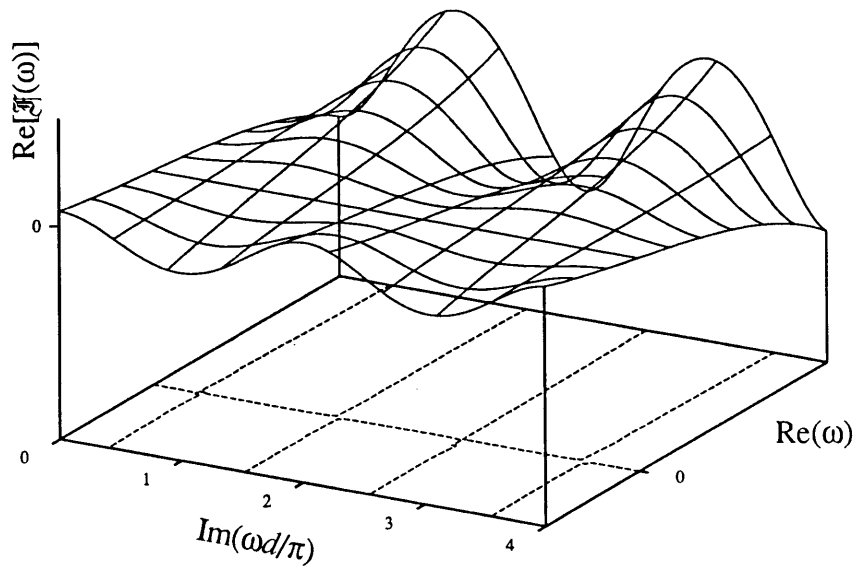

Figure 3.5. The real part of the function $\mathcal{F}(\omega) = 1/Q_1 - 1/Q_2$. The dotted lines give the values of ω for which $\mathrm{Re}(\mathcal{F}) = 0$. The value of the breakdown parameter $\chi = I_{slow}/I$ is 0.4.

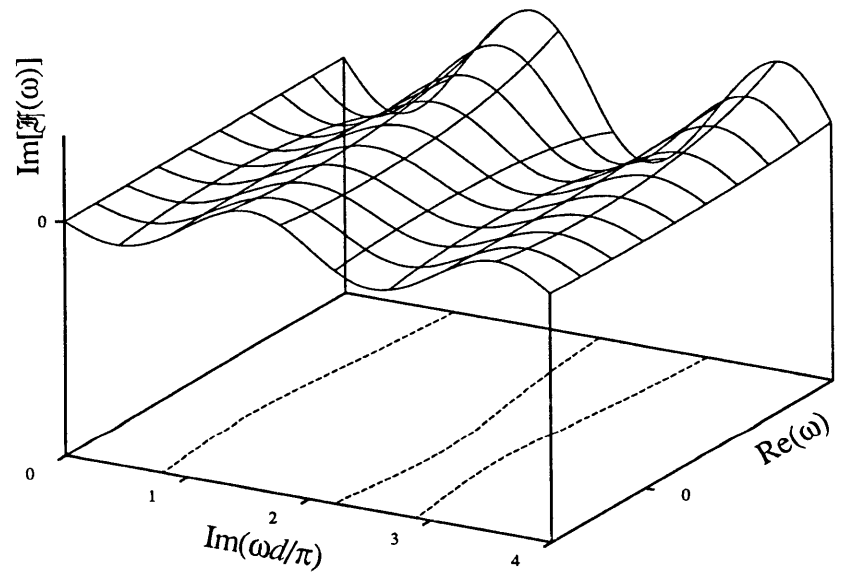

Figure 3.6. The imaginary part of the function $\mathcal{F}(\omega) = 1/Q_1 - 1/Q_2$, at the same value of χ. The dotted lines give the values of ω for which $\mathrm{Im}(\mathcal{F}) = 0$.

An alternative way to examine the eigenvalues in this discharge regime is illustrated in figure 3.7. Here the imaginary parts of both $1/Q_1$ and $1/Q_2$ are plotted as functions of Im(ω) for Re(ω) = 0. These functions are given by

$$\mathrm{Im}[1/Q_1(\omega)] = \frac{\sin(\omega_I d)}{\cos(\omega_I d) - \exp(\alpha_i d)}, \qquad \omega_R = 0 \tag{3.92}$$

and

$$\mathrm{Im}[1/Q_2(\omega)] = \frac{-\omega_I}{\alpha_i + \left(\omega_I^2 + \alpha_i^2\right)/\alpha_m \gamma_m S(d)}, \qquad \omega_R = 0, \tag{3.93}$$

where the more compact notation ω_I, ω_R has been used in place of Im(ω) etc. (Note that both $\mathrm{Re}(1/Q_1)$ and $\mathrm{Re}(1/Q_2)$ are equal to zero where Re(ω) = 0.) The eigenvalues ω_j occur where these two curves cross in figure 3.7. Clearly the number of solutions is infinite; in the limit of large j the eigenvalues are approximated by

$$\omega_j \sim \mathrm{i}\frac{j\pi}{d}. \tag{3.94}$$

This implies that the decay rates of the higher order terms in equation (3.82) approach the natural or free decay rates discussed in section 3.1.

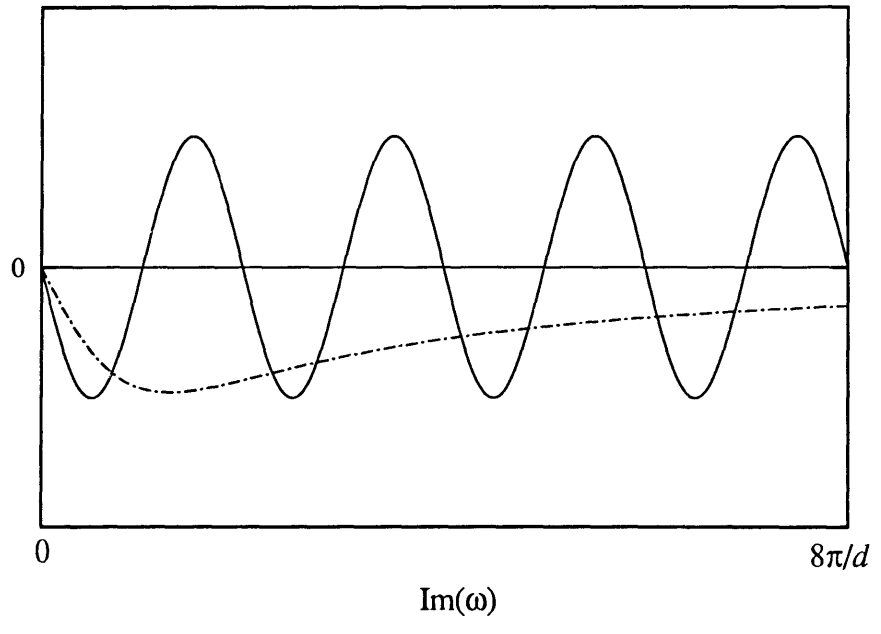

Figure 3.7. The functions $\mathrm{Im}[1/Q_1(\omega)]$ (solid line) and $\mathrm{Im}[1/Q_2(\omega)]$ (chained line) for Re(ω) = 0. Here the breakdown parameter $\chi = 0.4$.

Note that the apparent solution at $\omega = 0$ is a consequence of the fact that both Q_1 and Q_2 are proportional to $1/|\omega|$ at small values of $|\omega|$. A plot of the function $\mathrm{Re}(\omega Q_1 - \omega Q_2)$ which appears in figure 3.11 shows no such zero.

In the case of argon at this pressure and field, some of the eigenvalues become complex-valued nearer to breakdown. This is illustrated in figures 3.8, 3.9 and 3.10. Here the discharge parameters are identical to those used to calculate the previous three diagrams, except that χ has been raised to the value of 0.6. In an experiment this would normally be achieved by changing either the electrode spacing, the pressure or the electric field, but for simplicity it has been done here by increasing the nominal value of $\alpha_m\gamma_m$. It can be seen in figure 3.10 that the second minimum in $\mathrm{Im}(1/Q_1)$ along the imaginary axis no longer intersects the other curve. The zero-value lines in figures 3.8 and 3.9 now cross at points away from the imaginary axis. Eigenvalues ω_2 and ω_3 have therefore ceased to be purely imaginary and have become complex valued numbers which are symmetrically disposed about the imaginary axis. From equation (3.79), this implies that $T_2 = T_3^*$. Other pairs of eigenvalues may suffer a similar fate as the breakdown parameter is further increased, but only a finite number: this is because, even at breakdown, the trend of equation (3.93) is toward zero for large values of $\mathrm{Im}(\omega)$, whereas $\mathrm{Im}(1/Q_1)$ (equation 3.92) maintains a constant amplitude.

From equations (3.87) and (3.89), it can be seen that $Z(\omega) = Z^*(-\omega^*)$. Therefore, in the event that $\omega_3 = -\omega_2^*$ as described above, equation (3.81) becomes

$$N_m(z,t) = B_1 Z_1(z)\exp(-t/T_1) + \sum_{j=4}^{\infty} B_j Z_j(z)\exp(-t/T_j)$$

$$+B_2 Z_2(z)\exp(-t/T_2) + B_3 Z_2^*(z)\exp(-t/T_2^*). \qquad (3.95)$$

It is clear that B_3 must equal B_2^* for N_m to be real-valued. In this case, the expression for N_m becomes

$$N_m(z,t) = B_1 Z_1(z)\exp(-t/T_1) + \sum_{j=4}^{\infty} B_j Z_j(z)\exp(-t/T_j)$$

$$+2\exp[-t\,\mathrm{Re}(1/T_2)]\{\mathrm{Re}[B_2 Z_2(r)]\cos[t\,\mathrm{Im}(1/T_2)] + \mathrm{Im}[B_2 Z_2(r)]\sin[t\,\mathrm{Im}(1/T_2)]\}. \qquad (3.96)$$

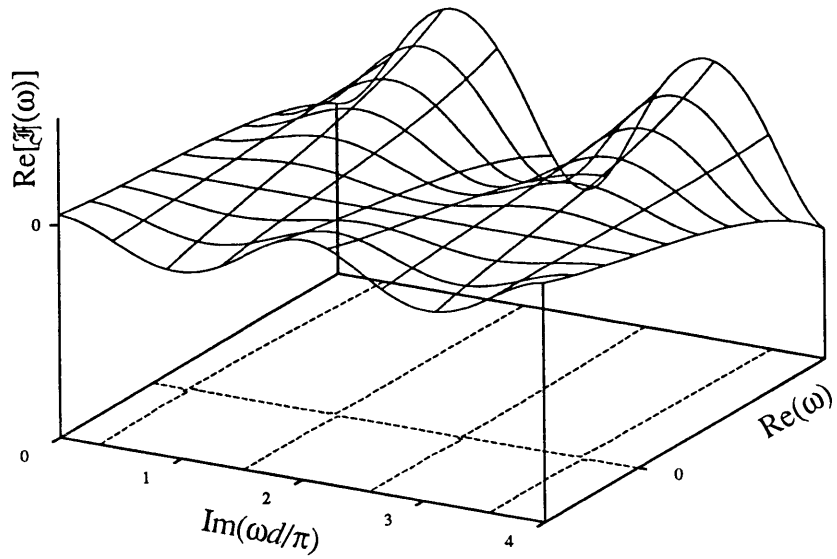

Figure 3.8. Same as figure 3.5, except the breakdown parameter $\chi = I_{slow}/I$ has here been given the value of 0.6.

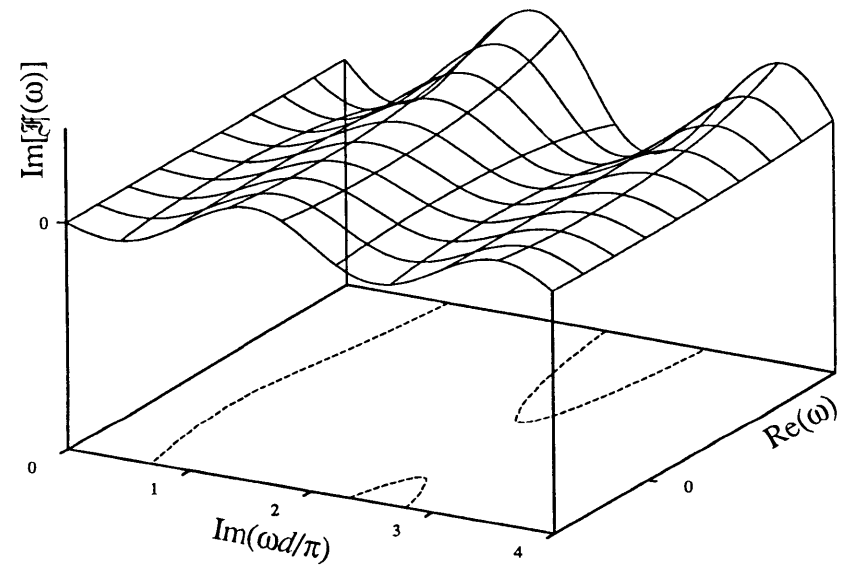

Figure 3.9. Same as figure 3.6, except that the breakdown parameter $\chi = I_{slow}/I$ has here been given the value of 0.6. A comparison with figures 3.5 and 3.6 shows that eigenvalues ω_2 and ω_3, which previously had values of about $(0 + 2.25\ i\ \pi/d)$ and $(0 + 2.75\ i\ \pi/d)$ respectively, are now approximately equal to $(\pm\omega_R + 2.5\ i\ \pi/d)$.

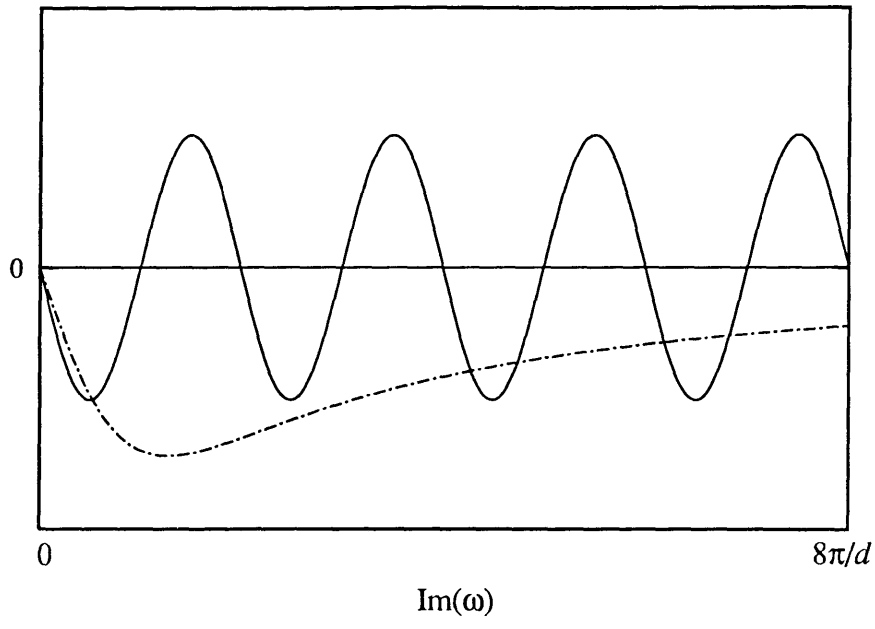

Figure 3.10. Same as figure 3.7, except that the breakdown parameter χ has here been given the value of 0.6. The second minimum of $\mathrm{Im}(1/Q_1)$ no longer dips below $\mathrm{Im}(1/Q_2)$; hence eigenvalues ω_2 and ω_3 have become complex-valued, leading to an oscillatory term in the expression for the decay of the 'slow' current.

Equation (3.96) is real-valued and therefore physically meaningful. If conditions are such that more eigenvalues become complex, their imaginary-valued contributions to equation (3.82) will cancel in the same way. This is because the symmetry of $\mathrm{Im}(\mathfrak{F})$ and $\mathrm{Re}(\mathfrak{F})$ with respect to the imaginary axis means that complex eigenvalues always occur in pairs such that $\omega_j = -\omega_{j+1}^*$.

At the point where a particular pair of eigenvalues become degenerate, the time-varying parts Θ of the corresponding two terms in equation (3.81) are both given by

$$\Theta(t) = (A + Bt)\exp\left[-t\,\mathrm{Re}(1/T)\right], \tag{3.97}$$

where A and B are constants. This corresponds to a critically damped, exponentially decaying sinusoid. The amount of oscillation may be described by the value of the 'quality factor' $\mathfrak{Q}$ (here given a script font to distinguish it from the quantity Q in equations 3.89 and 3.90), which is defined by

$$\mathfrak{Q} = \frac{\sqrt{\mathrm{Re}^2(1/T) + \mathrm{Im}^2(1/T)}}{2\,\mathrm{Re}(1/T)}. \tag{3.98}$$

Clearly $\mathfrak{Q}$ is equal to 1/2 at the point of degeneracy. At greater values of the breakdown parameter χ, as the real part of ω grows larger, the value of $\mathfrak{Q}$ increases and the oscillatory part of the decay becomes more evident. There is a limit to the size of Re(ω), however. The real and imaginary parts of $1/Q_1$ are given by

$$\mathrm{Re}\left(\frac{1}{Q_1}\right) = \sinh(\omega_R d)\left[\cosh(\omega_R d) - e^{\alpha_i d}\cos(\omega_I d)\right]/\Delta \tag{3.99}$$

and

$$\mathrm{Im}\left(\frac{1}{Q_1}\right) = \sin(\omega_I d)\left[\cos(\omega_I d) - e^{\alpha_i d}\cosh(\omega_R d)\right]/\Delta, \tag{3.100}$$

where

$$\Delta = \left[\cosh(\omega_R d)\cos(\omega_I d) - \exp(\alpha_i d)\right]^2 + \left[\sinh(\omega_R d)\sin(\omega_I d)\right]^2. \tag{3.101}$$

The quantity $1/Q_1$ therefore has singularities at ω such that

$$\cosh(\omega_R d) = \exp(\alpha_i d) \tag{3.102}$$

and

$$\omega_I = \frac{n\pi}{d}, \tag{3.103}$$

where n is an integer. Although a proof is not attempted here, it appears unlikely that zeros in $\mathfrak{F}$ can occur at values of ω_R greater than the singular value, because both Re($1/Q_1$) and Im($1/Q_1$) increase as some power of exp($\omega_R d$) at large ω_R. Similarly, the imaginary part of the smallest complex zero cannot be smaller than $2\pi/d$. The quality factor, and therefore the amount of oscillation, will therefore have a maximum value for a given value of the ionisation coefficient α_i. A greater degree of oscillation in the 2nd and 3rd decays may therefore be expected at high pressures and fields, where α_i is larger.

The coefficients B_j can be evaluated by Fourier expansion of the eigenfunctions $Z_j(z)$ (Ernest 1995b). In these terms, the expression for N_m at $t = 0$ becomes

$$N_m(z,0) = \sum_{k=1}^{\infty}\sum_{j=1}^{\infty} B_j C_{jk} \sin\left(\frac{k\pi z}{d}\right). \tag{3.104}$$

However, $N_m(z,0)$ can be independently expanded in a Fourier expansion (given by equation 3.60 with $t' = t$). Equating the coefficients of the same sine functions gives

$$A_k = \sum_{j=1}^{\infty} B_j C_{jk} \tag{3.105}$$

for each k. Approximate values of the B_j coefficients can be obtained by truncating this sum and inverting the resulting matrix equation.

In the breakdown limit, the value of the first time constant T_1 ought to increase without bound. Equation (3.79) implies that ω_1^2 should approach μ^2 in this limit, which means that the first eigenvalue ω_1 must become real-valued at some point. In figures 3.5 to 3.10, ω_1 remains imaginary in value. However, at greater values of the breakdown parameter χ, the changeover does take place. This is illustrated in figure 3.11.

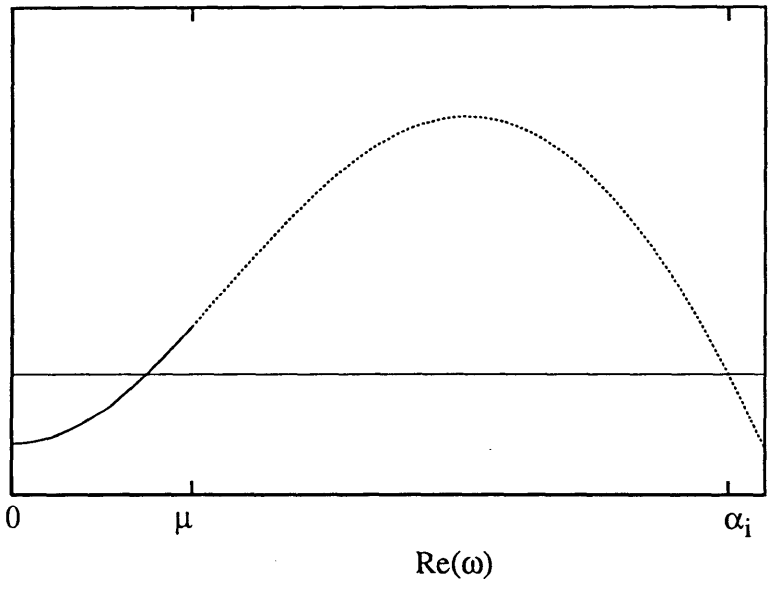

Figure 3.11. The function $\mathrm{Re}[\omega Q_1(\omega) - \omega Q_2(\omega)]$ for $\mathrm{Im}(\omega) = 0$. Physical values of ω are restricted to the solid part of the curve.

In this figure, the real part of ωQ_1 - ωQ_2 is displayed as a function of Re(ω), for Im(ω) = 0. (Im(ωQ_1 - ωQ_2) is equal to zero in this range of values of ω.) The eigenvalues ω_k are the zeros of this function. The same parameters were used to calculate these curves as were used for figures 3.5 to 3.10, except χ is here equal to 0.95. The first eigenvalue is seen to be real valued under these circumstances. (Note that one of the zeros in this figure is a 'fake' solution, corresponding to the case of $\omega = \alpha_i$, where it has already been noted that equation (3.87) is invalid.)

3.2.2.4. Complex components in Molnar's analysis.

It is of interest to see whether it is possible to extract complex time constants from Molnar's analysis. Suppose the rise of slow current is approximated by keeping three terms of equation (3.65). Equation (3.67), truncated at three terms, becomes a cubic equation,

$$\sum_{j=0}^{3} a_j T^j = 0, \tag{3.106}$$

where the a_j are constants. This must be solved to find the approximate values of the first three time constants $T_{1\text{-}3}$. It is well known that polynomials of order greater than one may have complex zeros, but note also that, if T is a zero of equation (3.106), then so is T^*; complex zeros must therefore occur in conjugate pairs. Without going into details, then, we can say that, for some values of the coefficients a_j, equation (3.106) has one real-valued zero and one conjugate pair of complex-valued zeros. Let this be the case, with $T_2 = T_3^*$ taken to be the conjugate pair. In order to evaluate the amplitudes $I_{s,j}$, we must invert the system

$$b_{kj} I_{s,j} = \frac{I_0 S(d) + I_{s0}}{\nu_k}, \quad j,k = 1 \text{ to } 3,. \tag{3.107}$$

where

$$b_{kj} = \left(\nu_k - 1/T_j\right)^{-1}. \tag{3.108}$$

The identity $T_2 = T_3^*$ implies that the column vector b_{k2} is the conjugate of b_{k3}. The matrix of b coefficients can be made real-valued by performing some column operations. The equation that results can be written as

$$\begin{bmatrix} b_{k1} \\ b_{k2}+b_{k2}^{*}=\mathrm{Re}(b_{k2}) \\ -\mathrm{i}\left(b_{k2}-b_{k2}^{*}\right)=\mathrm{Im}(b_{k2}) \end{bmatrix} \cdot \begin{bmatrix} I_{s,1} \\ I_{s,2}+I_{s,3} \\ \mathrm{i}\left(I_{s,2}-I_{s,3}\right) \end{bmatrix} = \frac{I_0 S(d)+I_{s0}}{\nu_k}; \qquad (3.109)$$

Since it is clear from this that both $I_{s,2}+I_{s,3}$ and $\mathrm{i}\left(I_{s,2}-I_{s,3}\right)$ must be real-valued, the implication is that $I_{s,2}=I_{s,3}^{*}$. The expression for the rise of 'slow' current (equation 3.65) therefore becomes

$$I_{\mathrm{slow}}(0,t)=I_{s,0}-I_{s,1}\exp(-t/T_1)-I_{s,2}\exp(-t/T_2)-I_{s,2}^{*}\exp\left(-t/T_2^{*}\right); \qquad (3.110)$$

once again, the imaginary parts of the complex terms cancel, leaving a real-valued expression which includes an oscillatory term, similar to equation (3.96).

As mentioned in section 3.2.1, the amplitudes $I_{s,j}$ in equation (3.65) generally decrease rapidly with j. The exception to this rule occurs if a pair of eigenvalues ω_j and ω_{j+1} are close to the point where they change from imaginary to complex values. At the changeover point, the eigenvalues, and therefore the time constants T_j and T_{j+1}, become degenerate. At this point the matrix of coefficients in equation (3.68) becomes singular. It is reasonable to expect that the amplitudes $I_{s,j}$ and $I_{s,j+1}$ might grow large (although of opposite sign) in the approach to this point of degeneracy.

3.2.2.5. Discharge regimes in which complex zeros occur.

It is of interest to investigate the discharge regimes in which complex time constants occur in the expression for the decay of current. This is, in general, a difficult task, because equations (3.89) and (3.90), which the eigenvalues ω_j must jointly satisfy, are complicated functions of many variables. The analysis is, however, much simpler in the breakdown limit. As this limit is approached, the parameter $\alpha_m\gamma_m S_d$ increases monotonically; this trend causes the right-hand side of equation (3.93) to also increase for any given value of Im(ω). The effect of this increase on the nature of the eigenvalues can be seen in figures 3.7 and 3.10. It is clear, therefore, that complex eigenvalues will occur

in the breakdown limit if they occur at all. At breakdown, the function $\mathfrak{G}(\omega) = Q_1 - Q_2$ has the form

$$\mathfrak{G}(\omega) = \left[\omega\frac{\cosh(\omega d_{bd}) - \exp(\alpha_i d_{bd})}{\sinh(\omega d_{bd})} + \alpha_i\right]\left(\mu^2 - \alpha_i^2\right)$$

$$-\left[\mu\frac{\cosh(\mu d_{bd}) - \exp(\alpha_i d_{bd})}{\sinh(\mu d_{bd})} + \alpha_i\right]\left(\omega^2 - \alpha_i^2\right). \quad (3.111)$$

If $\mathrm{Re}(\omega) = 0$, the real part of $\mathfrak{G}$ is also zero, and

$$\mathrm{Im}[\mathfrak{G}(\omega)] = \left[\omega_I\frac{\cosh(\omega_I d_{bd}) - \exp(\alpha_i d_{bd})}{\sinh(\omega_I d_{bd})} + \alpha_i\right]\left(\mu^2 - \alpha_i^2\right)$$

$$+\left[\mu\frac{\cosh(\mu d) - \exp(\alpha_i d)}{\sinh(\mu d)} + \alpha_i\right]\left(\omega_I^2 + \alpha_i^2\right). \quad (3.112)$$

Note that this equation can be couched purely in terms of the parameters ω_I/μ, α_i/μ and μd_{bd} (d_{bd} being the electrode separation at breakdown). The values of the zeros of equation (3.112) will therefore be functions of these parameters only. Now, the parameters α_i/μ and μd_{bd} also offer a convenient way to display the important features of a particular discharge environment. From equation (2.10), the breakdown separation d_{bd} is related to α_i by

$$\alpha_i d_{bd} \sim \alpha_i d_0 + \ln[1 + 1/\gamma], \quad (3.113)$$

where the generalised secondary coefficient $\gamma = \overline{\omega}(d)/\alpha_i$. The logarithm of γ is a slowly varying function of d_{bd}; if d_0 is relatively small, then, a plot of α_i/μ against $1/\mu d_{bd}$ at various values of the reduced electric field *E/N* should fall approximately along a straight line for a given combination of gas and cathode material. The slope depends mainly upon the value of $\overline{\omega}(d)$, which is closely related to the secondary coefficients γ_i and γ_m (see equation 2.31). Hence, the greater the activity of the cathode material, the lower the slope of the resulting line.

Plots of α_i/μ against $1/\mu d_{bd}$ at different *E/N* are displayed in figure 3.12. Equation (3.112) has also been analysed to determine the values of α_i/μ and μd_{bd} at which the

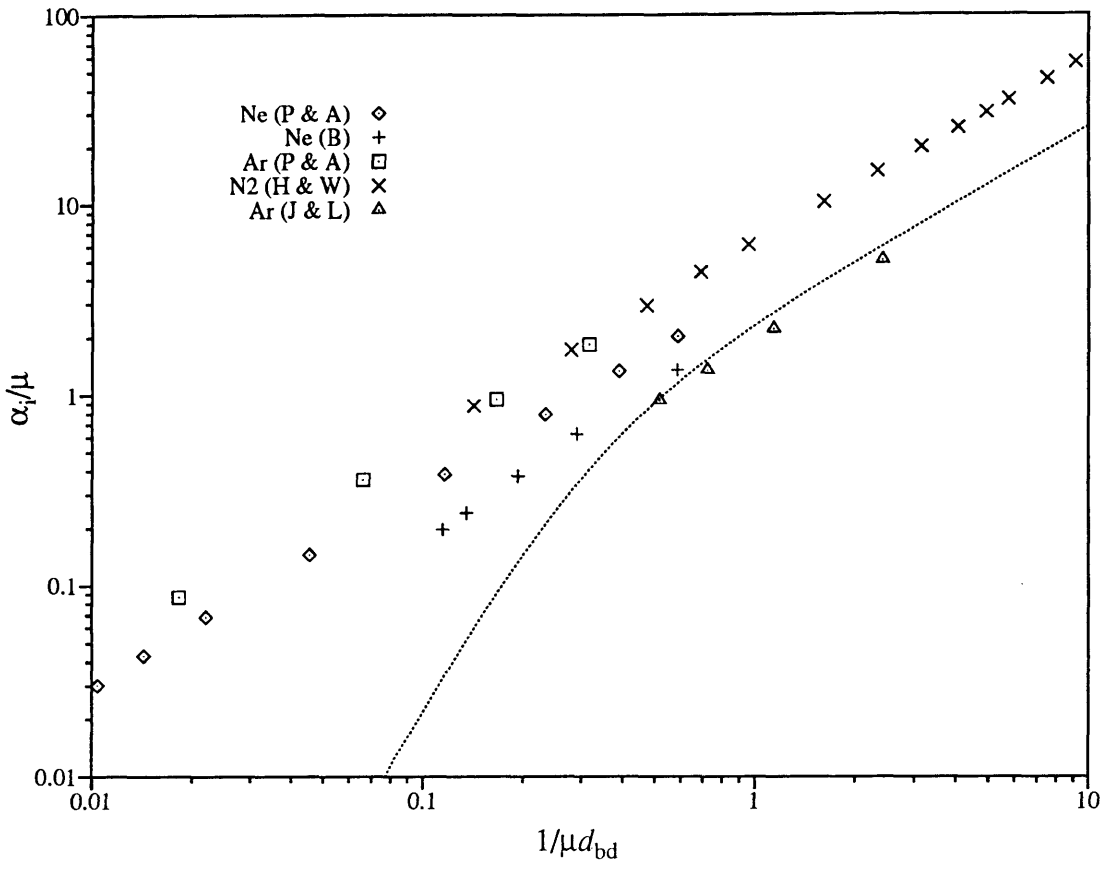

Figure 3.12. This diagram illustrates the occurrence of oscillatory terms in the series that describes the decay of 'slow' current. The area above and to the left of the dotted line indicates the region where such terms occur in the breakdown limit. The plotted points represent the electrode separation at breakdown (d_{bd}) of a gas at a given value of ionisation coefficient α_i and diffusion parameter μ. The parenthetised letters in the legend refer to the source of the d_{bd} data for that particular gas: 'P & A' stands for Penning and Addink (1934); 'B', for Brunker (1984); 'H & W', for Haydon and Williams (1976); and 'J & L', for Jacobs and Larocque (1946). The α_i and μ values were obtained from the following: Kruithof and Penning (1937) and Dielis *et al* (1979) (neon); Kruithof (1940) and Ellis and Twiddy (1969) (argon); Haydon and Williams (1976) and Levron and Phelps (1978) (N_2).

second and third decay time constants change from real to complex values at breakdown. The dotted line marks the boundary between the 'real' and 'complex' regions of the graph. Both the neon and the argon data of Penning and Addink (1934) were measured in a chamber with an iron cathode; Haydon and Williams (1976) used a gold cathode, whereas Brunker (1984) used one made of copper. The final data set, taken from Jacobs and LaRocque (1946), was measured in a discharge against a barium cathode. These authors measured the variation in breakdown voltage V_{bd} with pd in an argon discharge using three different cathode materials: aluminium, magnesium and barium. Barium produced the smallest value of V_{bd} at the Paschen minimum, so was presumably the material which

had the largest secondary emission coefficients. It can be seen that only these last data lie in the region of the graph where all the decay constants are real-valued. (This does not necessarily imply that the results of Haydon and Williams (1976) and Brunker (1984), both of whom used the Molnar analysis to reduce their data, are in error. The situation even a small way from breakdown may be very different.)

3.3. Conclusion.

Two types of time-resolved experiment have been discussed in this chapter. The first of these is the 'free decay' experiment, in which the concentrations of excited states are allowed to decay without regeneration. Because the modelling of these decays is a straightforward diffusion problem which has been understood for some time, only a brief recapitulation has been presented here. However, conditions at the boundary, particularly in the low-pressure limit, are not so well understood. In section 3.1.1 of the present chapter, an expression was derived relating the coefficient β in the boundary condition to the fraction R of metastable particles reflected from a boundary without quenching. This analysis employed a more detailed model of the velocity distribution among the metastable particles near the wall than has been incorporated in any previously published treatment. However, the resulting expression is at odds with experiment, since it predicts that R should be on the order of some tens of percent, whereas experimental values of this quantity are orders of magnitude smaller (Conrad *et al* 1982a, b). Clearly more work, both experimental and theoretical, needs to be done on distributions of metastables near an absorbing boundary.

In the second type of time-resolved experiment, there is a partial regeneration of the concentrations of excited states, which is achieved by the maintenance of a potential difference between the electrodes after the cessation of the source of primary current. This potential difference allows a weighted sum of the concentrations of all excited states to be determined by measuring the current passed by the decaying discharge afterglow. Unfortunately, the regeneration term complicates the analysis of this experiment. Molnar (1951a) has described a treatment in which the diffusion equation was transformed to an integral form. This author concluded that the slow decay in discharge current could be described by an infinite sum of exponentials. A brief recapitulation of Molnar's theory was presented in section 3.2.1. In the section following this, an alternative analysis involving the separation of variables technique was described. Ernest has presented a similar

discussion (Ernest 1995a), in which he raised the possibility that some of the decay time constants may become complex-valued under some discharge conditions.

It can therefore be seen that Molnar's analysis is incomplete. In particular, some of the decay rates may become complex-valued near to breakdown, leading to the appearance of exponentially damped sinusoidal terms in the slow decay of the discharge current. Figure 3.12 indicates that this is likely to occur if the cathode material is not very amenable to the ejection of secondary electrons. Some experimental results are presented in chapter 9 that are, broadly speaking, consistent with this prediction. However, the match is not perfect: in particular, the predicted value for the decay rate of the second term in the sum in equation (3.65) is very different from the experimentally measured value (see figure 9.10). The theory as described in section 3.2.2 is also mathematically quite complicated. It is not yet clear which terms in these equations are most important. Further work should examine whether any approximations can be made to the theory which would allow the articulation of the physics in a simpler mathematical form.